ADVANCING EARTH AND SPACE SCIENCES

JGR Earth Surface

RESEARCH ARTICLE
10.1029/2024JF007968

Network-Scale Dynamics of Alluvial Cover in a Mixed Bedrock-Alluvial River

Mel Oliveira Guirro[1], **Rebecca Hodge**[1], **Fiona Clubb**[1], **and Laura Turnbull**[1]

[1]Department of Geography, Durham University, Durham, UK

Key Points:

- Model effectively simulated broad network-scale alluvial cover patterns
- Slope is a primary control on alluvial cover distribution and expansion, particularly in supply-limited conditions
- Alluvial cover extent is highly responsive to sediment supply and discharge, especially in supply-limited conditions

Supporting Information:

Supporting Information may be found in the online version of this article.

Correspondence to:

M. O. Guirro,
mel.oliveira-guirro@durham.ac.uk

Citation:

Guirro, M. O., Hodge, R., Clubb, F., & Turnbull, L. (2025). Network-scale dynamics of alluvial cover in a mixed bedrock-alluvial river. *Journal of Geophysical Research: Earth Surface*, *130*, e2024JF007968. https://doi.org/10.1029/2024JF007968

Received 1 AUG 2024
Accepted 13 FEB 2025

Author Contributions:

Conceptualization: Mel Oliveira Guirro, Rebecca Hodge, Fiona Clubb, Laura Turnbull
Data curation: Mel Oliveira Guirro
Formal analysis: Mel Oliveira Guirro
Funding acquisition: Rebecca Hodge, Fiona Clubb, Laura Turnbull
Methodology: Mel Oliveira Guirro, Rebecca Hodge, Fiona Clubb, Laura Turnbull
Project administration: Rebecca Hodge, Fiona Clubb, Laura Turnbull
Supervision: Rebecca Hodge, Fiona Clubb, Laura Turnbull
Visualization: Mel Oliveira Guirro
Writing – original draft: Mel Oliveira Guirro

Abstract Limited understanding of how sediment cover varies spatially in mixed bedrock-alluvial river networks inhibits our comprehension of erosion processes in these systems. This study investigates the complex interactions between channel and sediment properties that control the extent, spatial distribution, and connectivity of alluvial cover in mixed bedrock-alluvial river networks. Employing a combination of field data, sediment transport modeling, and connectivity analysis, this study aims to understand the key drivers influencing sediment cover patterns at the network scale. Sediment transport simulations using the NetworkSedimentTransporter model explored how varying initial fluvial and channel parameters affect the steady-state alluvial cover across the River Carron network in the Scottish Highlands. The results demonstrate that increased initial sediment cover, increased sediment supply, and larger grains increased the extent and connectivity of alluvial sections, whereas deeper flow reduced them. In supply-limited conditions, the spatial distribution of alluvial cover is most sensitive to slope, while in transport-limited conditions, sediment supply and grain size become more critical. Even at high sediment supply rates, not all reaches achieved full alluviation, suggesting inherent limitations in sediment distribution. Additionally, channel slope was the most significant factor controlling the directional growth of alluvial sections. These findings contribute to the limited research on the controls of alluvial cover at the network scale, thereby improving our understanding of landscape evolution, river management, and habitat conservation of mixed bedrock-alluvial rivers.

Plain Language Summary Rivers can have their bedrock exposed, be covered by sediment, or a mix of both. Understanding how sediment cover changes across river networks is important for predicting erosion, managing rivers, and protecting habitats. This study used a computer model to simulate sediment movement in the River Carron network in Scotland. We explored how factors such as initial sediment cover, water depth, sediment supply, and grain size affect sediment distribution. We found that more initial sediment, higher sediment supply, and larger grains increased sediment cover, while deeper water reduced it. Even with a high sediment supply, exposed bedrock persisted in some areas. Slope was the main factor controlling where sediment accumulated, especially when sediment supply was low. However, sediment supply became more important in controlling where sediment accumulated when supply was high. Our study highlights the complex interaction of factors shaping river landscapes and provides insights for better river management and conservation strategies.

1. Introduction

River channels can be predominantly alluvial, characterized by sediment deposits covering the riverbed and banks, or bedrock, where exposed rock is present in the channel bed or banks. Bedrock rivers control landscape evolution because river incision into bedrock sets the hillslope base level (Whipple et al., 2013). Some river systems comprise a combination of bedrock exposure and sediment-covered patches, termed mixed bedrock-alluvial river systems. In this context, alluvial cover refers to areas covered in sediment regardless of the underlying bedrock's elevation. While continuous long bedrock channels are relatively rare, mixed bedrock-alluvial river systems are relatively common worldwide (Whipple et al., 2013). The alluvial cover of river channels is the result of complex interactions between hydraulics and sediment transport processes. These interactions play a crucial role in the evolution of rivers, influencing ecosystems, river engineering, and shaping the terrestrial features around them.

Fluvial discharge and sediment supply play major roles in controlling alluvial cover. A higher discharge increases the shear stress and sediment transport rate (Ferguson, Sharma, Hardy et al., 2017; Ferguson, Sharma, Hodge et al., 2017). However, large rainfall events can trigger a larger sediment supply, leading to greater potential for

Writing – review & editing: Mel Oliveira Guirro, Rebecca Hodge, Fiona Clubb, Laura Turnbull

alluvial cover development or bedrock incision (Cook et al., 2020; DeLisle & Yanites, 2023; Turowski et al., 2013). When sediment supply is low, increasing it can lead to more frequent impacts of grains on the bed, increasing erosion. However, as the sediment supply continues to increase, it eventually forms continuous alluvial cover, protecting the underlying bedrock from erosion. These processes are known as the "tools and cover" effect and the balance between them is critical in determining whether a reach will incise or develop alluvial cover (Sklar & Dietrich, 2004; Turowski et al., 2007).

Understanding these complex interactions is important because transitions between bedrock and alluvial reaches impact the location of bedrock incision within the channel and affect sediment connectivity, that is, the degree to which sediment can move through the system without being retained in transient storage zones (Fryirs, 2013). These factors can alter the patterns of alluvial erosion and deposition across the river network. The extent of alluvial cover is typically predicted based on the relative sediment flux, which is the sediment supply rate relative to the bed load transport capacity (Chatanantavet & Parker, 2008; Inoue et al., 2014; Johnson, 2014; Sklar & Dietrich, 2004). However, flume and field experiments have shown that several stable cover fractions can form for a given sediment supply-to-transport capacity ratio depending on bed roughness, antecedent alluvial cover, channel geometry, and entrainment probability (Chatanantavet & Parker, 2008; Hodge et al., 2011). Discharge and sediment supply are extrinsic parameters influenced by regional climate, tectonics, and hillslope processes including landslides. These controls exhibit complex interactions across diverse spatial and temporal scales, challenging the prediction of the spatial patterns and evolution of bedrock and alluvial reaches.

Channel geometry, including slope, width, and depth, influences alluvial cover by affecting flow dynamics and sediment transport. Steeper slopes and narrower channels generally increase shear stress and promote sediment transport. Bedrock channels are typically expected to be narrower, deeper, and steeper than alluvial channels for a given drainage area (Montgomery & Gran, 2001; Whitbread et al., 2015). However, when sediment flux is restricted, bedrock channels may be wider and shallower than alluvial channels (Buckley et al., 2024; Meshkova & Carling, 2013; Whitbread et al., 2015) and may be found in low-slope reaches (Jafarinik & Viparelli, 2020). The transport capacity of a channel, which is influenced by its geometry, fluctuates with changes in discharge (Sklar & Dietrich, 1998). This dynamic relationship creates a feedback loop between form and function: channel morphology affects sediment transport, while sediment dynamics shape the channel through processes of bedrock erosion and sediment deposition (Baynes et al., 2020; Johnson & Whipple, 2010; Turowski, 2018). Consequently, channel morphology and sediment transport are interlinked. However, a comprehensive understanding of this feedback is still lacking, particularly in mixed bedrock-alluvial reaches.

The presence of sediment cover in mixed bedrock-alluvial channels affects transport processes, with the fraction of sediment cover affecting grain entrainment, transport, and deposition. Previous work has shown that sediment particles tend to travel between sediment patches and deposit in those patches, creating a positive feedback mechanism (Ferguson, Sharma, Hardy et al., 2017; Ferguson, Sharma, Hodge et al., 2017; Hodge et al., 2011). Grain characteristics, such as grain size and shape, also influence alluvial cover in mixed bedrock and alluvial systems. In bedrock reaches, sediment can be transported across bedrock patches independently of grain size due to smoother bed surfaces and fewer particle-particle interactions. Transport in alluvial channels is more size-selective due to rough bed surface and complex particle interactions such as grain hiding, which also increases critical shear stress (Hodge et al., 2011). However, exceptionally large particles, such as glacial erratics, may not be easily transported in bedrock reaches (Whitbread et al., 2015). In bedrock channels, sediment patches tend to initially cluster in lower-slope areas and near other larger grains; that is, the riverbed morphology and large grains influence the formation of sediment patches, which in turn can affect subsequent development of channel morphology (Goode & Wohl, 2010; Hodge & Hoey, 2016).

Despite extensive research on individual bedrock-alluvial reaches, our understanding of sediment transport dynamics and controls on alluvial cover at the network scale remains limited. Most previous studies have explored alluvial cover controls in single reaches at shorter timescales, typically months, without considering larger spatial and temporal scales. These studies include flume experiments (Chatanantavet & Parker, 2008; Hodge & Hoey, 2016; Johnson & Whipple, 2010; Papangelakis et al., 2021), field analysis (Ferguson, Sharma, Hardy et al., 2017; Ferguson, Sharma, Hodge et al., 2017; Finnegan et al., 2017; Hodge et al., 2011; Inoue et al., 2014; Rennie et al., 2018; Turowski et al., 2008), or modeling (Jafarinik & Viparelli, 2020; Johnson, 2014; Lague et al., 2005; Turowski, 2018). To address this gap in understanding, it is essential to examine the feedback

Journal of Geophysical Research: Earth Surface 10.1029/2024JF007968

mechanisms between discharge, sediment supply, channel geometry and grain characteristics and their effects on alluvial cover dynamics at both reach and network scales.

Sediment connectivity within river networks is a critical concept that determines the transport efficiency and depositional patterns of sediments, influencing both small- and large-scale processes (Bracken et al., 2015; Schmitt et al., 2016). Within this context, alluvial patches act as these transient storage zones by increasing the residence time of sediments and reducing their availability for downstream transport (Czuba & Foufoula-Georgiou, 2015). In contrast, bedrock reaches tend to facilitate faster sediment transport, enhancing connectivity by minimizing sediment retention. Therefore, the distribution and characteristics of bedrock and alluvial reaches within a river network are expected to directly influence the temporal and spatial dynamics of bedload sediment connectivity. Furthermore, the direction of the alluvial patch expansion, whether upstream or downstream, is expected to vary in response to environmental conditions, such as sediment supply, flow dynamics, channel geometry, and sediment characteristics. By understanding sediment connectivity, we can explore how feedback mechanisms between channel form and sediment transport processes operate across different scales, providing insights into how small-scale processes affect large-scale patterns.

Recent sediment transport models, such as CASCADE (Schmitt et al., 2016; Tangi et al., 2019) and Network-SedimentTransporter (Czuba, 2018; Pfeiffer et al., 2020), reproduce sediment transport processes at a network scale, providing a comprehensive understanding of sediment connectivity and transfer within river systems. These models track bed load sediment particles in the river system, depending on the hydraulics, grain characteristics, and channel morphology of the reaches. Studies have used these models to analyze the effect of sediment pulses in river networks (Ahammad et al., 2021; Czuba & Foufoula-Georgiou, 2014; Gran & Czuba, 2017), hotspots for fluvial geomorphic change (Czuba & Foufoula-Georgiou, 2015), spatiotemporal changes in bed sediment thickness (Czuba et al., 2017), dam effects on sediment transport dynamics (Schmitt et al., 2018), wildfire sediment cascades (Murphy et al., 2019) and to discriminate between multi- and single-channel patterns (Bizzi et al., 2021). However, none of these studies have explored patterns of alluvial cover in a mixed bedrock-alluvial river network, despite the importance of sediment cover for landscape evolution (Whipple & Tucker, 2002), river management (Toone et al., 2014), and habitat conservation.

This study aims to clarify the complex interactions among primary controls on alluvial cover within mixed bedrock-alluvial river networks by employing a combination of field data from the River Carron in the Scottish Highlands, network scale modeling using NetworkSedimentTransporter, and connectivity analysis. We use field data to parameterize the model and evaluate its performance. We create several scenarios to assess how changing sediment supply, flow depth, and grain size affect the alluvial cover patterns at the network scale. Finally, we conducted a connectivity analysis to evaluate cover transitions, fragmentation, and expansion of alluvial reaches.

2. Study Area

We focus on the River Carron in the northwest of the Scottish Highlands (Figure 1), a mixed bedrock-alluvial river system with available data on alluvial cover fraction, bankfull channel width, channel slope, channel depth, and discharge (Whitbread, 2015; Whitbread et al., 2015). The catchment area is 300 km^2. The total river network is approximately 138 km long, while the main River Carron is 44 km. Bedrock reaches are generally narrower, deeper, and steeper than alluvial reaches in this system (Whitbread et al., 2015).

The Carron catchment has a history of glaciation, with the most recent glacial activity occurring during the Last Glacial Period, ending approximately 11 ka ago (Ballantyne, 2008). The bedrock lithologies in this region exhibit moderate to high resistance to erosion. They are mainly composed of metamorphosed sandstone (psammite and pelite) with granite in the southeast region (British Geological Survey, 2008). The superficial deposits in the catchment are mainly of glacial origin, including till and glaciofluvial sediments. However, there are localized regions covered by organic peat near the rivers and mass movement deposits near the toes of hillslopes. The main sources of sediment supply to the rivers are alluvial deposits situated in proximity to the channels, including raised alluvial terraces and debris fans associated with tributary streams, and infrequent landslides in the catchment.

3. Methods

We used a combination of field data collection (Section 3.1), sediment transport modeling (Section 3.2), and connectivity analysis (Section 3.3) to investigate controls on the spatial distribution of sediment cover, using the

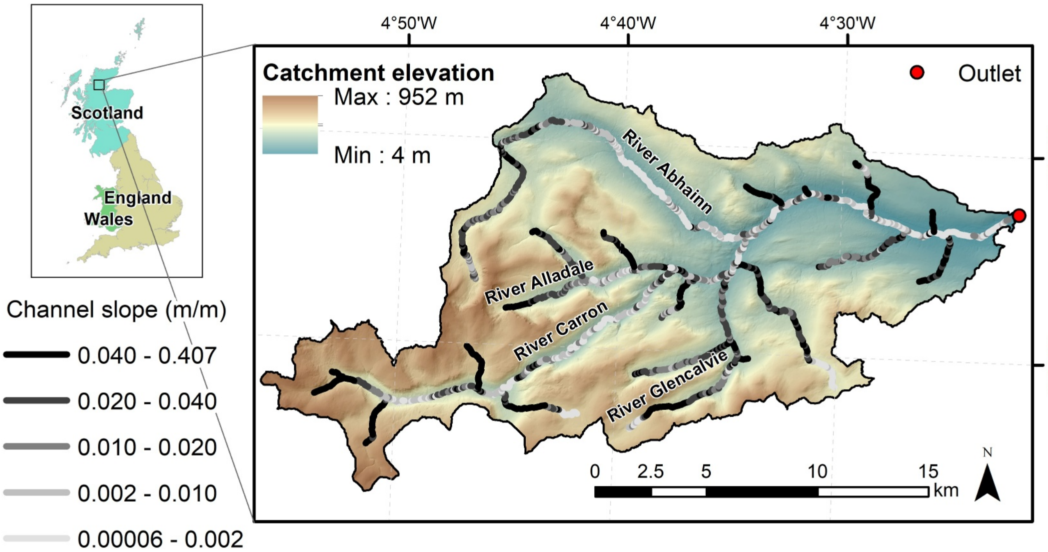

Figure 1. Elevation map of the Carron catchment and channel slope of the river network (white = low slope; black = high slope). The inset map shows the location of the Carron catchment in the Scottish Highlands.

River Carron as a representative river network. Field data were used to approximate input parameters for the sediment transport model, which we used to explore how varying initial sediment cover, discharge, sediment supply, and grain size affected steady-state sediment cover across the network. Model outputs were compared with field data and analyzed using statistical and connectivity metrics.

3.1. Data Sources and Field Data Collection

Channel morphology data collected by Whitbread (2015) in 2010–2011 provide measurements of sediment cover percentage, channel width, and depth for the River Carron's main channel. Further field data on grain size and sediment cover percentage were collected in September 2022 for the main channel and eight other tributaries. Grain size distributions were determined by analyzing at least three photos from each of 91 gravel bars using the automated mode of PebbleCounts (Purinton & Bookhagen, 2019). The median grain size (D_{50}) across all bars was used as the default model grain size. It was found that the automatic mode of PebbleCounts decreased D_{50} by 3 mm compared to manual analysis. However, this uncertainty in the D_{50} was considered acceptable for this study, and therefore, the automatic mode was used. Sediment cover percentage was estimated in 41 reaches, each with a length of approximately 200 m. The average alluvial cover was visually estimated along 11 transects spaced every 20 m for each reach. In total, sediment cover data were collected for approximately 8 km of the channel. The sediment cover data from Whitbread (2015) and the percentage of alluvial cover collected in 2022 were used to evaluate the performance of the alluvial cover fraction resulting from the sediment transport modeling. The detailed data set collected in 2022, including site locations, grain size (D_{50} and D_{84}), and sediment cover data, is available in Guirro et al., 2025.

3.2. Sediment Transport Simulations

Network scale sediment transport simulations were conducted to analyze how varying initial sediment cover, discharge, sediment supply, and grain size affect the extent and spatial distribution of alluvial cover in a river network at steady state. The NetworkSedimentTransporter model (Pfeiffer et al., 2020) is a physically based model that simulates the transport and evolution of sediment parcels through a river network over time. Sediment parcels are individual units representing a group of particles with identical characteristics, such as grain size. The model tracks the movement of these parcels. Key outputs are changes in parcel locations, bed elevation, and bed slope over time. This capability facilitates the analysis of bedload sediment connectivity within the river network.

To set up the NetworkSedimentTransporter model, the river network, represented as a grid of links (river segments) and nodes (initial and end points of river segments), was constructed using the LSDTopoTools topographic analysis software package (Mudd et al., 2023) and a 5-m resolution Digital Elevation Model (DEM)

10.1029/2024JF007968

sourced from the OS Terrain 5 (Ordnance Survey, 2022). A minimum drainage area threshold of 2.5 km^2 was defined to create the river network. A link length of approximately 100 m was used as this length captures the shortest bedrock reach observed in the field by Whitbread (2015). The river network was manually adjusted at the outlet based on aerial imagery due to poorly constrained channel locations in the low-slope DEM region. Other node and link parameters required by NetworkSedimentTransporter, such as node elevations, link lengths, and drainage areas, were also defined using the DEM and LSDTopoTools (Mudd et al., 2023). Link widths and depths were derived from power-law scaling relations based on drainage area and bankfull data from the River Carron (Whitbread et al., 2015), accounting for 86% of the spatial variation in channel width and 61% of the variation in channel depth.

The NetworkSedimentTransporter model was implemented using the open-source code (available on Github: github.com/landlab/landlab). We modified the original model to better represent the transport dynamics and to estimate the spatial distribution of alluvial cover. Four key adaptations were implemented.

The first adaptation was the determination of the percentage of the alluvial cover of each river segment. The alluvial cover develops on a non-erodible bed, with the elevation defined by the topographic elevation from the DEM. Sediment parcels with a volume of 1 m^3 were added on top of the non-erodible bed. On average, 194 parcels were required to achieve 100% coverage of one-grain diameter deep at each river segment. A fully alluvial reach can be 100% covered or more, creating layers of alluvial cover. The alluvial cover percentage (p_c) for a given river segment or link (l) was calculated using Equation 1:

$$p_c = \frac{V_l}{l_l \times W_l \times D_l \times (1 - \varphi)} \times 100 \tag{1}$$

where p_c is the alluvial cover percentage in link l; V_l is the volume of sediment parcels in link l (m^3); l_l is the link length (m); W_l is the link width (m); D_l is the average median grain size of sediment parcels in link l; and φ is the bed porosity, which was set as 0.3. This equation does not consider the spatial distribution of alluvial cover within a reach and the effect of bed roughness on alluvial cover.

The second modification of the model was the creation of a function to add sediment parcels into the system at each timestep. This function allows the choice of the location (river segment) to which parcels are added. In the simulations, parcels were added at the second-most upstream links in all tributaries. The most upstream link was not chosen because the upstream node elevation is fixed, preventing the links from adjusting their slope and transporting sediments. Adding sediments to the second-most upstream link allowed the slope to adjust freely and transport sediments to downstream links. To avoid boundary effects, the two most upstream links of each tributary were excluded from further analysis.

The third modification was that a minimum transport capacity in low slope links was set to prevent bottleneck issues and ensure that the simulations could achieve a steady state in a reasonable time, that is, in less than 2 weeks of CPU time. It was enforced that links with slopes lower than 0.002 m/m, which represent 20% of the river network, would have more than 100% cover and a transport capacity at least equal to the sediment input. This modification kept the sediment cover realistic and did not break the sediment connectivity in the system due to artificial bottlenecks. A similar approach of setting a minimum transport capacity to prevent bottleneck issues was taken by Czuba et al. (2017) and Gran and Czuba (2017).

Finally, the downstream sediment parcel movement function was modified to update the parcel velocity and transport capacity for each link traversed by a parcel. Without this modification, grains originating in steep links would maintain their high velocities even when transiting through flatter downstream links, and thus traverse unrealistically long distances within a single timestep. The updated approach recalculates velocity for each link, reflecting varying hydraulic conditions, and reassesses transport capacity as parcels exit a link. These improvements prevent sediment parcels from unrealistically skipping across links, thereby improving the connectivity analysis and representation of sediment dynamics in river networks. However, the sediment transport processes are the same regardless of whether the reach is bedrock or alluvial.

The model operates by iterating through timesteps, moving parcels downstream and adjusting bed topography. The timestep length was defined as one day for the simulations. The model dynamics for each timestep is as follows:

Table 1
Parameter Values Used in the Simulations

Parameter	Default value rationale	Default value	Values simulated
Initial sediment cover	200% due to the sensitivity analysis	194 parcels/reach on average	1%, 10%, 25%, 50%, 75%, 90%, 100%, 200%, 500%
Flow depth	Bankfull depth (H_b)	1.8 m on average	0.25 H_b, 0.5 H_b, 0.75 H_b, H_b, 1.25 H_b, 1.5 H_b, 1.75 H_b, 2 H_b
Sediment supply	Average transport capacity (Q_t) across all reaches	60 parcels/tributary	0 Q_t, 0.02 Q_t, 0.1 Q_t, 0.2 Q_t, 0.4 Q_t, 0.8 Q_t, Q_t, 1.25 Q_t, 1.7 Q_t, 2.5 Q_t, 3.3 Q_t
Grain size	Median grain size (D_{50}) measured in the field	0.10 m	0.3 D_{50}, 0.5 D_{50}, 0.7 D_{50}, D_{50}, 1.3 D_{50}, 1.5 D_{50}, 1.7 D_{50}

Note. The default values are common to all simulations apart from when the impact of that parameter is being investigated. The specific values evaluated for the initial sediment cover, flow depth, sediment supply, and grain size were modified separately for different simulations.

1. Add sediment parcels into the second-most upstream link or each tributary.
2. Define active and inactive sediment parcels based on grain size and flow conditions, according to Wong et al. (2007). Active parcels determine the active layer thickness from which parcels will be entrained.
3. Calculate the reach slope based on bed topography, which considers both bedrock topography and alluvial depth.
4. Move active parcels downstream according to the parcel velocities calculated using the Wilcock and Crowe (2003) sediment transport equation. This equation relates the dimensionless transport rate of each parcel to the ratio of bed shear stress, calculated by slope-depth product, to the reference shear stress. The reference shear stress represents the critical shear stress required to initiate motion for the parcel grain size, adjusted by the effects of the median grain size of the bed surface. In our implementation, we calculated the reference shear stress using a constant dimensionless reference Shield stress of 0.036. This value was achieved by setting the Wilcock-Crowe sand fraction parameter to zero, a simplification justified by our field observations showing low sand presence (Supporting Information S1).
5. Update the parcel location of active parcels, which will change bed elevation and reach slope in the next timestep.
6. Calculate the alluvial cover percentage of each reach (Equation 1).

Further details on the model dynamics and model derivation can be found in Czuba (2018) and Czuba et al. (2017).

An initial exploration assessed model sensitivity to initial sediment cover by analyzing its effect on the final percentage of alluvial cover of reaches at steady state. The initial sediment cover was varied from 1% to 1,000% (average depths of 0.01–10 times D_{50}, forming up to 10 layers of alluvial cover). After the sensitivity analysis, simulations were performed until the steady state to investigate how parameters (initial sediment cover, flow depth, sediment input, grain size) impacted the percentage of alluvial cover on the network scale (Table 1). Parameters were varied individually from default values, which were initially approximated using field data for realistic scenarios, although not aiming to reproduce exact field conditions. A reach was considered to be in a steady state if the alluvial cover varied by less than 10% in 100 timesteps. Some reaches displayed regular periodic fluctuations in the sediment cover. These links are in a dynamic equilibrium but were not included in the previous steady state definition of cover changing by less than 10% in 100 timesteps. Therefore, the system was considered to be in a steady state when the number of reaches in the steady state remained constant for 100 timesteps. On average, 78% of the reaches achieved this condition in each run. To contextualize our NetworkSedimentTransport model results at steady state, we also developed a zero-order model based on transport capacity for comparison. This simpler model assumes full alluviation when a reach's transport capacity exceeds the sediment supply. Details of this comparison are provided in the Supporting Information S1.

The default initial sediment cover for the simulations of 200%, that is, cover depth is twiceD_{50}, was chosen based on the sensitivity analysis results comparing the final percentage of alluvial cover across multiple model runs with varying initial sediment covers. Simulations starting with initial sediment covers of 200% or more found similar final alluvial cover percentages, indicating stability. In contrast, simulations with initial sediment cover below 200% showed substantial variability in the final percentage of alluvial cover, demonstrating sensitivity to the initial conditions. We therefore included initial sediment cover in our analysis.

The default value of flow depth was set to bankfull depth, as D_{50} is expected to be mobile under bankfull conditions. Bankfull depth for each reach was estimated according to the power law channel geometry scaling relations to drainage provided by Whitbread (2015) for the River Carron. The model does not enforce flow continuity between links because depth is specified independently per link without verifying the consistency of inflows and outflows. The model focuses on tracking sediment transport and bed topography evolution rather than full hydrodynamic routing (Czuba et al., 2017).

The default value of sediment supply was set to match the average transport capacity of the system, which is a critical threshold for sediment cover dynamics. This average transport capacity was calculated by taking the mean of the transport capacities of all reaches in the network during the first timestep, using the Wilcock and Crowe equation as implemented in the model. This calculation considered only the initial bedrock topography, not accounting for potential changes in slope due to sediment deposition. A range of simulations with low sediment supply (less than transport capacity) and high sediment supply (greater than transport capacity) were then tested (Table 1). Sediments were added at the top of all tributaries, instead of from hillslopes, representing sediments coming from upstream reaches and so focusing on simulating river network sediment dynamics. The number of sediment parcel input per timestep was constant across all tributaries, reflecting that they all have the same upstream catchment area. Here, we use the terms “supply-limited” and “transport-limited” to describe network-scale conditions rather than individual reach states. When the network sediment supply is less than the average transport capacity, we consider the network “supply-limited”, although individual reaches may still be transport-limited. Conversely, when sediment supply exceeds average transport capacity, we consider the network “transport-limited”, although some reaches may remain supply-limited. This approach allowed us to analyze how the network-scale alluvial cover adjusts as the overall sediment supply changes relative to the network's average transport capacity.

The default value of the grain size was equal to the D_{50} measured in the field, which was 0.1 m. Simulations were performed with a uniform grain size distribution. The parcel volume was set as 1 m^3. No abrasion rate was defined, that is, sediments did not lose size or volume when transported. The sediment density was 2,650 kg/m^3, and the starting location of parcels in each link was randomly defined, which is the only random parameter in the model. Four runs of the default simulation, varying only the random starting location of parcels, verified that this randomness can alter the total alluvial length in the network by ±2%.

Alluvial cover results from all simulations were compared with field observations to assess the plausibility of the model outputs given the network's topology, rather than to precisely replicate field conditions. For the River Carron, data from Whitbread (2015) were used, while field data collected in 2022 were used for the tributaries. This comparison aimed to verify the model's ability to capture the general patterns of alluvial cover distribution within the river network. The Percentage Bias (PBIAS) was calculated to quantify the difference between the average simulated and average observed alluvial cover across the river network. The Root Mean Square Error (RMSE) and the Mean Absolute Error (MAE) quantified the error of the model's accuracy in a reach-by-reach analysis.

3.3. Analysis of Controls on the Alluvial Cover: Extension, Spatial Distribution, and Connectivity of the Alluvial Cover

For each simulation, we assessed how the extent and spatial distribution of alluvial cover varied to investigate the impact of initial sediment cover, flow depth, sediment supply, and grain size. Reaches were classified based on the percentage of alluvial cover at steady state: <10% cover as bedrock, 10%–99% cover as mixed, and >99% cover as alluvial. The <10% threshold for classifying reaches as bedrock was chosen to account for occasional transient sediment accumulation in bedrock reaches, ensuring that reaches with temporary cover were not misclassified as mixed.

The sequence of different reach types was examined by analyzing the order and transition of different riverbed categories along the river network. This involved mapping the transitions between bedrock, mixed, and alluvial reaches to understand the spatial progression of sediment cover types. By studying the frequency of these transitions, we identified patterns and factors that control the distribution and connectivity of sediment cover within the river system.

Sub-networks of each riverbed category (bedrock, mixed, alluvial) were created by selecting only reaches of the corresponding type from the overall river network. Within each sub-network, adjacent reaches of the same category were linked to form continuous sections using the weakly connected components algorithm from NetworkX (Hagberg et al., 2008; Available on Github: github.com/networkx/networkx). This algorithm identifies clusters of connected sections within the same category, allowing us to measure the total length of connected sections within the same category, and the number of these sections. This analysis provided insights into how varying channel and sediment properties influence the continuity and fragmentation of alluvial, bedrock and mixed reaches.

4. Results

4.1. Comparison of Simulation Results With Field Observation

The final alluvial cover from all simulations was compared with field observations (Figure 2). On a network scale, the simulation using the default parameter values specified in Section 3.2 (Figure 2b) exhibited the closest agreement to the field observation (Figure 2a), overestimating the total average amount of observed cover by an average of 1% (PBIAS = −1%). In contrast, the simulation with no sediment supply (Figure 2c) showed the poorest match with the field data (Figure 2a), underestimating the observed alluvial cover by an average of 40% (PBIAS = 40%). However, point-by-point comparisons revealed substantial local variance between simulations and the field data. Both the best-performing and worst-performing simulations showed a wide spread of errors at specific locations (Figures 2d and 2e). For the best-performing simulation, the RMSE was 0.48, and the MAE was 0.36. This result indicates that while the model accurately captured the average network-scale alluvial cover, its accuracy in predicting cover at discrete locations was limited. Despite these location-specific discrepancies, the model adequately represented the overall pattern of alluvial cover on the network and is thus suitable for investigating the processes controlling alluvial cover on a network scale.

In general, the simulations that closely matched the field observations had high values of initial sediment cover (>200%) and intermediate values of flow depths (1–1.5 bankfull depth), sediment supply (0.75–1.25 transport capacity), and grain size (0.75–1 times field D_{50}) (Figure 2f). Among these, sediment supply was the most influential parameter affecting model performance, with the no-supply simulation performing the worst compared to the field data.

4.2. Controls on the Alluvial Cover

The percentage of alluvial cover in the river network at steady state increased with higher initial sediment cover, sediment supply, and grain size (Figures 3a, 3c, 3d and 4), but decreased with increased flow depth (Figures 3b and 4). The proportion of alluvial reaches was most sensitive to flow depth, particularly when the depth was less than bankfull (Figure 4). The influence of flow depth exhibited a threshold behavior, with the greatest variations in sediment cover occurring when flow depth was less than bankfull depth (Figures 3b and 4). Beyond this threshold, additional increases in flow depth resulted in marginal changes in alluvial cover, highlighting the system's reduced sensitivity to excess flow depth. Grain size also demonstrated a threshold behavior (Figure 4). Below a critical size (around the median size of 0.1 m found in Carron catchment), smaller grain sizes severely limited the alluvial cover as they were easily transported downstream. Above this threshold, increases in grain size had a minor effect on further alluvial cover formation.

The overall increase in alluvial reaches with increasing sediment supply was gradual (Figure 4). However, the development of bedrock reaches (cover <10%) and mixed reaches (cover between 10% and 99%) showed a threshold behavior (Figure 3c). Simulations with low sediment supply, particularly below the river network's average transport capacity, resulted mostly in reaches with either 100% or 0% cover, inhibiting mixed reaches. As sediment supply increased toward the system's transport capacity, mixed reaches became more common. Beyond this threshold, further increases in sediment supply had a minor impact on the formation of bedrock, mixed and alluvial reaches (Figure 3c).

In addition to the total amount of sediment cover, analyzing its spatial distribution across the network is also important for understanding river system dynamics. Spatial variations in alluvial cover under distinct channel and sediment simulations revealed that higher initial sediment cover and supply, along with larger grain sizes and reduced flow depth, tended to increase the number of alluvial sections (Figure 5 and Supporting Information S1,

10.1029/2024JF007968

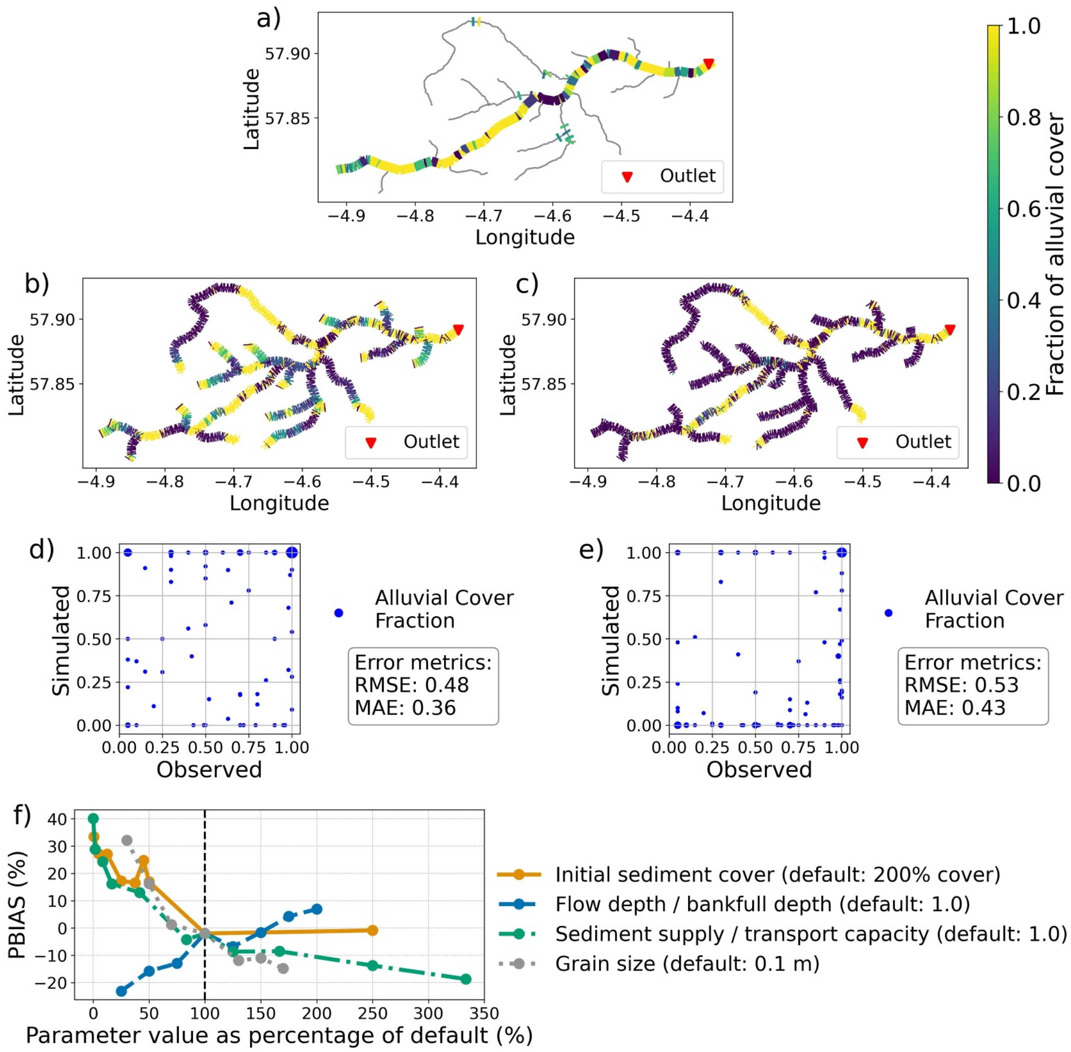

Figure 2. Comparison of model results and field observations. Spatial distribution of the alluvial cover fraction: (a) Observed in the River Carron (data from Whitbread, 2015, for the main channel, and fieldwork conducted in 2022 for tributaries); (b) Best-performing simulation, with default parameter values specified in Section 3.2 and PBIAS = −1%; (c) Worst-performing simulation, with no sediment supply and PBIAS = 40%. Scatter plots of the observed and simulated alluvial cover fraction for (d) best-performing and (e) worst-performing simulations. The size of the blue points indicates the number of reaches at each location, with larger points representing more reaches. The smallest point represents one reach, while the largest point represents 11 reaches. The root mean square error (RMSE) and the mean absolute error (MAE) quantify the error in the model's accuracy; (f) Percentage bias (PBIAS) fit between the average simulated alluvial cover fraction and the average observed field data for all simulations. A value of 100% on the *x*-axis indicates the parameter's default value, as detailed in the legend and Table 1. Values below or above 100% represent reductions or increases from this reference value, representing different simulations.

which provides videos demonstrating the variation in steady state sediment cover across the range of all parameter values). The threshold parameter value at which each river segment transitioned from a non-alluvial state in one run to an alluvial state in another run (defined as > 99% cover) was identified (Figure 6). Under extreme scenarios, such as minimum initial sediment cover, no sediment supply, smallest grain size, and highest flow depth, some alluvial reaches were still formed (Figure 6). As parameter values changed to favor sediment deposition, new alluvial segments were generally connected to existing alluvial reaches, leading to the elongation of continuous alluvial sections rather than the formation of additional small fragmented sections. This indicates that the growth in the total length of alluvial cover primarily occurs through the expansion of existing alluvial sections.

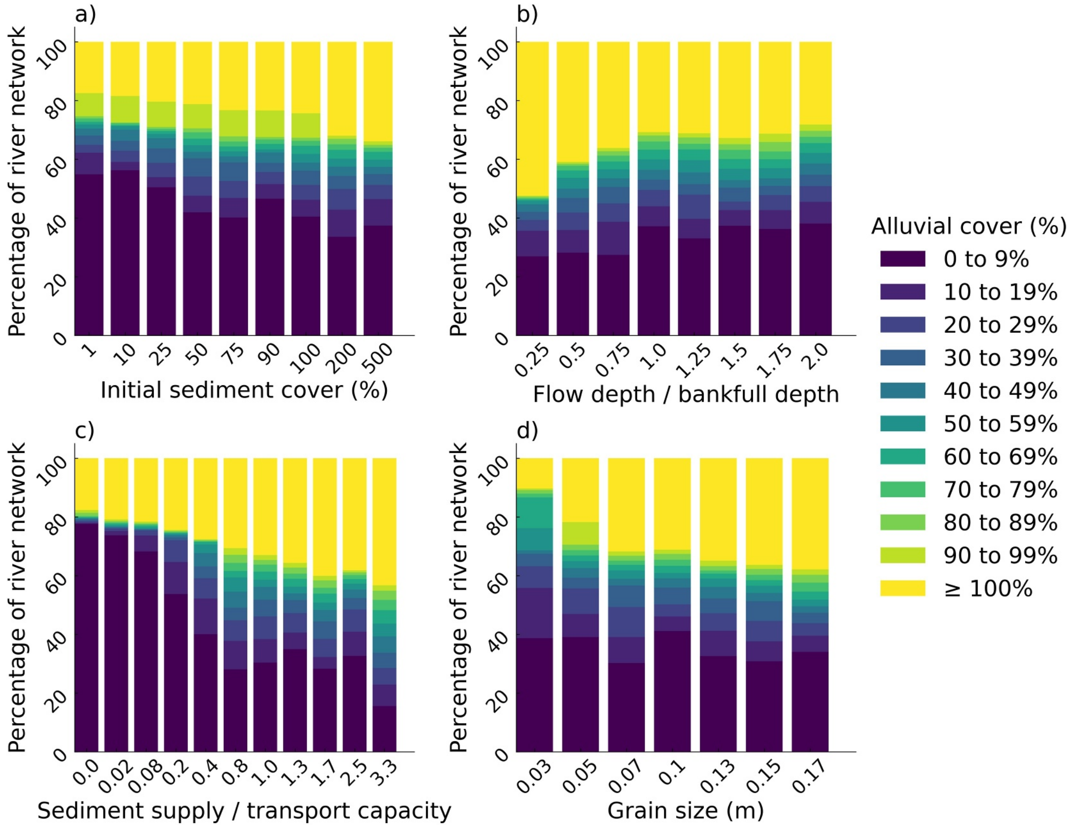

Figure 3. Influence of parameter values on alluvial cover in a steady-state river network. The analyzed parameters include: (a) initial sediment cover (e.g., 100% indicates a completely covered riverbed and 500% indicates a sediment depth equivalent to five times D_{50}); (b) flow depth relative to bankfull depth; (c) sediment supply in relation to the river network's average transport capacity; and (d) uniform grain size. Each bar represents a simulation outcome. All other parameters were maintained at default values. Note: The *x*-axis is unscaled.

To assess the controls on alluvial cover formation, we consider the slopes of reaches that developed alluvial cover in each simulation. The slopes of alluvial reaches (cover fraction >99%) were generally higher with decreased flow depth, increased sediment supply, larger grain size, and higher initial sediment cover (Figure 7). Threshold behavior was again observed, with lower sensitivity of alluvial reaches to slopes at flow depths exceeding bankfull and at sediment supplies exceeding transport capacity. The occurrence of steep alluvial reaches in the 0.03 m grain size simulation was due to the small number of alluvial reaches, which were primarily formed in the tributary heads due to their proximity to the sediment supply source.

Figure 8 complements Figure 7 by presenting the distribution of slopes of reaches that became alluvial (i.e., cover fraction >99%) compared to the simulation with the previous parameter value. The transition to an alluvial state occurred across a range of slopes, revealing distinct patterns between the different parameters (Figure 8). As sediment supply increased up to the transport capacity threshold, steeper reaches achieved alluvial cover (Figure 8c). However, beyond this threshold, additional sediment supply did not result in steeper reaches becoming alluvial, indicating that slope did not control the formation of new alluvial reaches once the transport capacity was exceeded. The relationship between flow depth and the slope of reaches achieving alluvial cover showed a complex pattern (Figure 8b). When starting from bankfull flow depth, decreasing flow depth facilitated the achievement of steady-state alluvial cover on steeper reaches (Figures 7b and 8b). However, this trend was not consistent at higher flow depths. For initial sediment cover values above 1%, there is a general trend of reaches with lower slopes attaining alluvial cover as initial sediment cover increases (Figure 8a). However, this relationship is not strictly monotonic, with some fluctuations observed, particularly between 75% and 100% initial cover. For grain size values above 0.03 m, increasing the grain size increased the slope of the additional alluvial

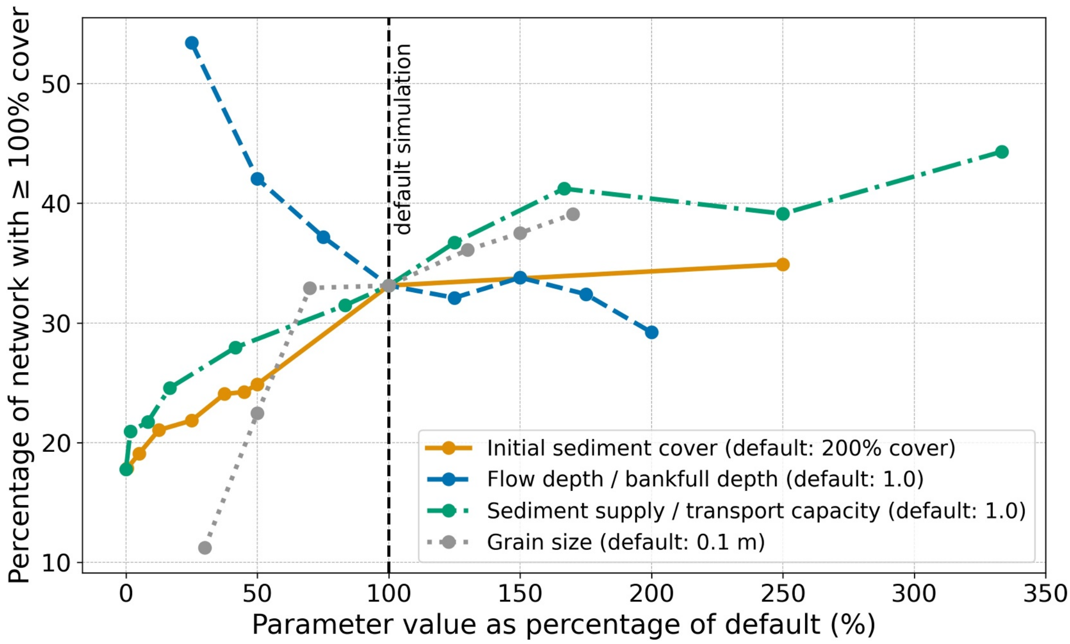

Figure 4. Sensitivity analysis of parameters influencing the percentage of network reaches with ≥100% alluvial cover. A value of 100% on the *x*-axis indicates the parameter's default value, as detailed in the legend and Table 1 and highlighted by the dashed vertical line. Values below or above 100% represent reductions or increases from this reference. Differences up to 2% in the percentage of network with ≥100% cover are in the range affected by the randomness of the model as discussed in Section 3.2.

reaches (Figure 8d). The patterns for initial sediment cover, flow depth, and grain size (Figures 8a, 8b, and 8d) were less pronounced compared to the clearer trend observed for sediment supply (Figure 8c).

The results show that channel slope is a determining factor in the formation of alluvial reaches (Figures 7 and 8). In general, decreasing flow depth and increasing initial sediment cover, sediment supply, and grain size caused increasingly steeper reaches to become alluvial. The slope played a critical role in controlling the locations of alluvial cover formation, especially when the sediment supply was below the river network's average transport capacity. For instance, with a sediment supply of 0.4 times the transport capacity, the median slope of alluvial reaches was around 0.0001 m/m, while at 0.8 times the transport capacity, the median slope increased to around 0.0005 m/m (Figure 7c). These findings demonstrate that steeper gradients can support greater sediment deposition when sediment supply is increased up to the transport capacity of the river. However, beyond the transport capacity threshold, other factors have a major influence on alluviation, as evidenced by the lack of further increase in the slope of alluvial reaches with additional sediment supply (Figure 8c).

4.3. Connectivity of Reach Cover Types

An important aspect of the spatial pattern of sediment cover is whether alluvial reaches are adjacent to other alluvial reaches or are more likely to alternate with bedrock sections. Analysis of the transition probabilities between adjacent upstream and downstream reaches showed that reaches were most likely to maintain their cover type between sequential 100 m reaches in each simulation (Figure 9). The probability of transitioning from bedrock to bedrock, mixed to mixed, or alluvial to alluvial reaches was around 80%, while the probability of transitioning between different cover types was generally lower than 20% (Figure 9). This low probability of transition between different reach types means that the total length of most alluvial, mixed, or bedrock sections was longer than 100 m. Transitions to another cover category were more common in simulations with low initial sediment cover, flow depth, sediment supply, and grain size. Specifically, low initial sediment supply and grain size values increased transitions from alluvial to mixed bedrock-alluvial reaches (AL to BR-AL), hindering the formation of long continuous alluvial sections (Figures 9a and 9d). Similarly, low flow depth and sediment supply values increased transitions from mixed bedrock-alluvial to bedrock reaches (BR-AL to BR), limiting the development of extensive mixed bedrock-alluvial sections (Figures 9b and 9c). Direct transitions from alluvial to

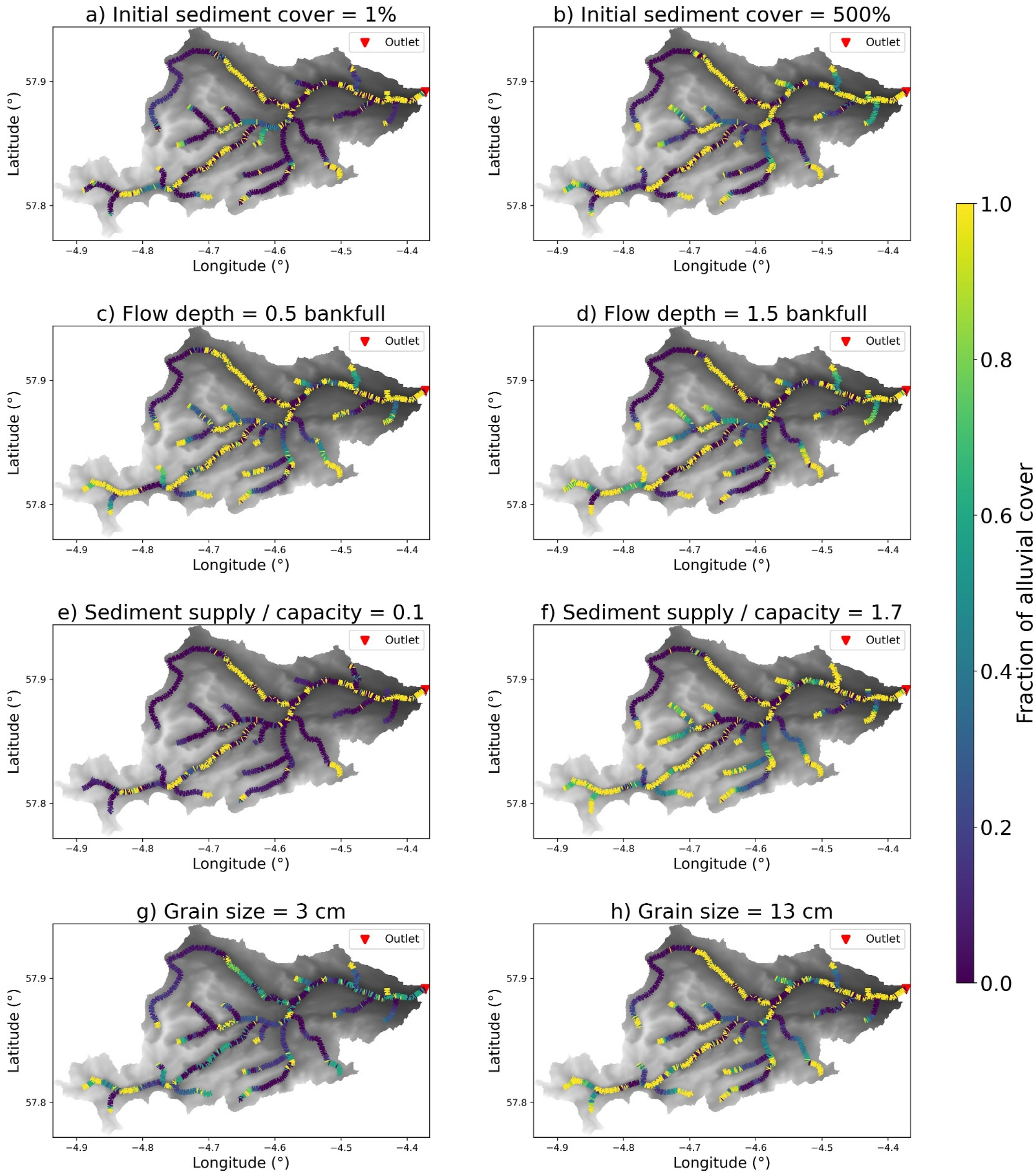

Figure 5. Spatial variations of the cover fraction at the steady state. Each figure indicates different parameter values: (a) low initial sediment cover (1%) versus (b) high initial sediment cover (500%, equivalent to five layers); (c) reduced flow depth (0.5 bankfull) versus (d) increased flow depth (1.5 bankfull); (e) limited sediment supply (0.1 of transport capacity) versus (f) high sediment supply (1.7 of transport capacity); and (g) small grain size (0.03 m) versus (h) large grain size (0.13 m). Elevation ranges from 4 m (in black) to 952 m (in white). Additional simulation results for all parameter values are presented in Supporting Information S1.

bedrock reaches or vice versa (AL to BR or BR to AL) were less common. The transition matrix for the default simulation is shown in Table 2.

The analysis of continuous cover section length and fragmentation across different cover types (bedrock, mixed, and alluvial) provides insights into the persistence and spatial organization of these sections within the river network (Figure 10). As initial sediment cover and sediment supply increased, the fragmentation of alluvial and mixed sections decreased, resulting in longer average lengths (Figures 10b and 10d). However, increasing sediment availability had contrasting effects on bedrock sections: initial sediment cover had minimal impact on average length (Figure 10b), while increased sediment supply significantly reduced bedrock section length from 1

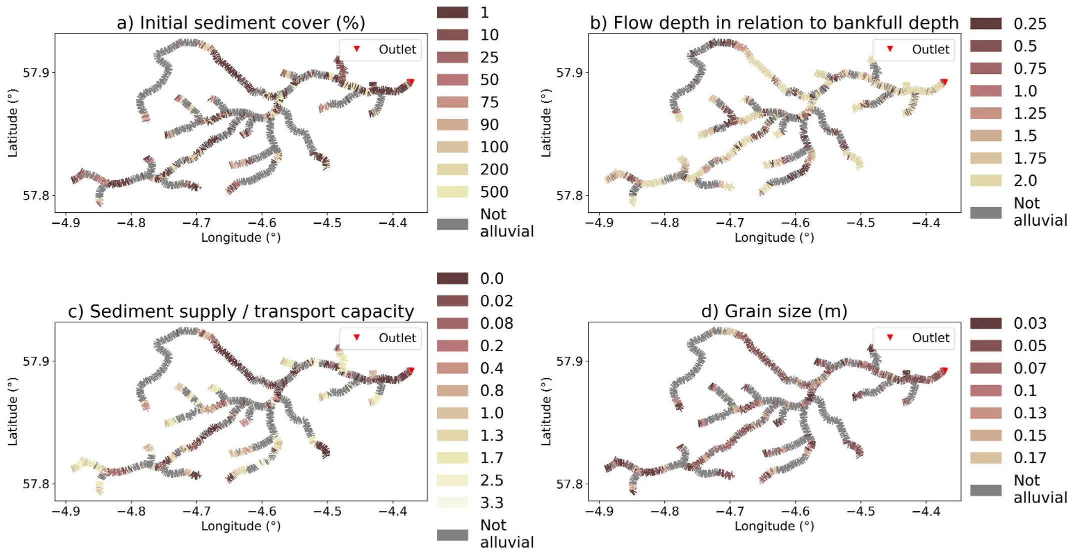

Figure 6. Threshold values of parameters required to achieve full alluviation (>99% cover) in each river segment, demonstrating how different reaches become fully alluvial at different parameter values. Each panel shows the threshold value for a different parameter: (a) initial sediment cover (%); (b) flow depth relative to bankfull depth; (c) sediment supply relative to transport capacity; and (d) grain size (m). The color of each river segment indicates the minimum parameter value at which that segment becomes fully alluvial. For example, in panel (a), dark brown segments become fully alluvial at just 1% initial cover, while lighter colors require higher initial cover to become fully alluvial. River segments labeled as "Not alluvial" (in gray) never achieved full alluviation under any simulated parameter value, indicating persistent bedrock exposure.

to 0.2 km on average (Figure 10d). Greater flow depths reduced the fragmentation of bedrock and mixed sections by increasing their length, while increasing the fragmentation of alluvial sections (Figure 10c). Grain size had minor effects on section characteristics compared with other parameters, with alluvial sections slightly lengthening with larger grains, while bedrock and mixed sections maintained relatively constant lengths (Figure 10e). These findings indicate that sediment availability and flow conditions are the main controls on the connectivity of cover sections, particularly the promotion of long bedrock sections under low sediment supply conditions. A similar connectivity analysis comparing the main River Carron field data to simulation results is presented in the Supporting Information S1, providing further information into the model's performance in replicating the observed cover patterns. This analysis shows that the model generally produced connectivity trends observed in the field, but it tended to produce shorter and more sections for all cover types compared to field observations.

The slope of the river profile and the sediment supply location control the direction of the alluvial extension between model runs (Figure 11). Alluvial sections predominantly expanded in the direction of increasing slope, producing downstream expansion in reaches with convex profiles (as highlighted by the dashed boxes in Figure 11) and upstream expansion in reaches with concave profiles (as highlighted by the dotted boxes in Figure 11). River segments characterized by uniform slope and no concavity displayed a tendency towards fragmented alluvial formation without a distinct direction in alluvial expansion. The longitudinal profiles further revealed that the sediment supply location in the most upstream reach of each tributary produced an elongation of alluvial sections in the downstream direction near headwater nodes. In the simulations tested, this upstream sediment supply location affected alluviation up to 2 km downstream when there was a high sediment supply.

5. Discussion

5.1. Spatial Distribution and Extent of Alluvial Cover

Our network-scale modeling reveals complex interactions between channel slope, discharge, and sediment supply that control the spatial distribution and extent of alluvial cover in mixed bedrock-alluvial river systems. These interactions can be understood through the concepts of transport-limited and supply-limited conditions, providing insights beyond previous reach-scale studies. We found that channel slope primarily controlled the spatial distribution of alluvial cover, especially when the network was under supply-limited conditions (Figures 6–8).

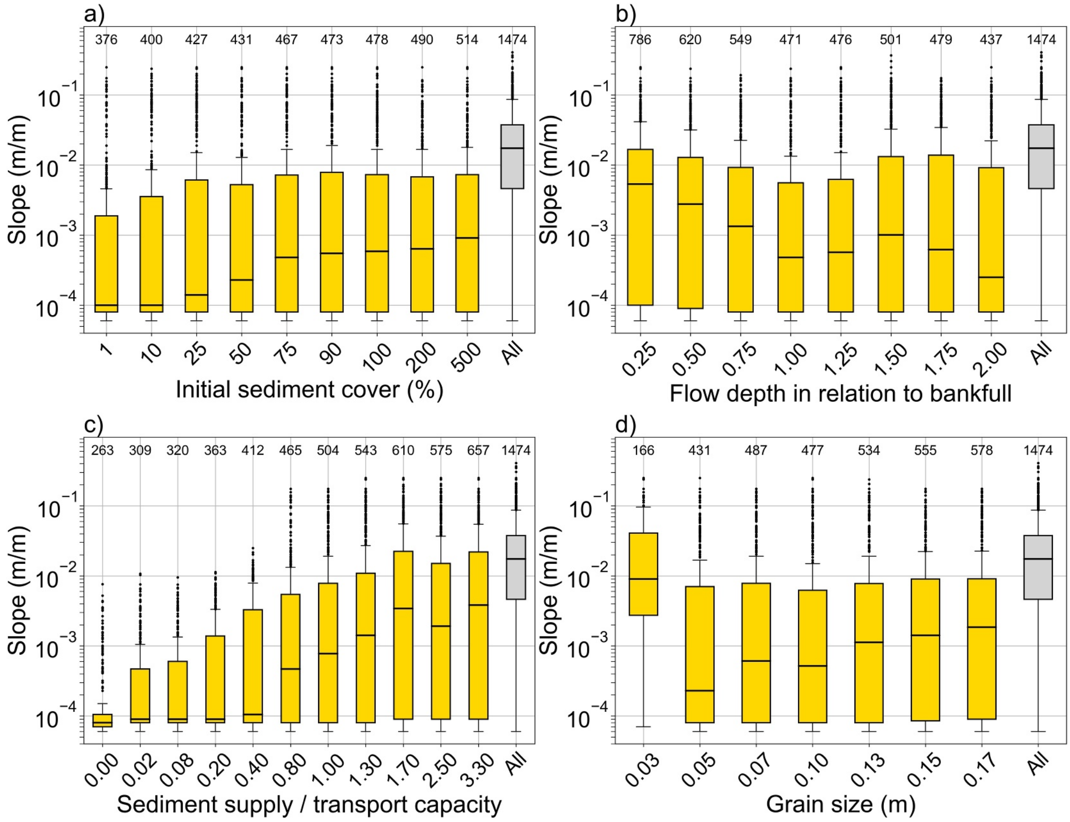

Figure 7. Channel slopes of all alluvial reaches (i.e., cover fraction >99%) for each simulation in steady state, when varying the parameters: (a) initial sediment cover; (b) flow depth relative to bankfull depth; (c) sediment supply relative to transport capacity; and (d) grain size. Each box plot represents a simulation initiated with the respective parameter value. All other parameter values were maintained at default values. The gray bar refers to the initial slope of all reaches in the network, which is independent of the simulation. The numbers at the top of each boxplot indicate the number of alluvial reaches.

Reaches with lower bedrock slopes were more likely to achieve alluvial cover, while steeper bedrock reaches remained sediment starved. This finding extends previous reach-scale studies that have also indicated preferential sediment deposition in topographic lows (Chatanantavet & Parker, 2008; Hodge & Hoey, 2016; Johnson & Whipple, 2010). Our network-scale approach demonstrates how these processes influence alluvial cover patterns across a full range of slope variations within an entire river network. We found that even under simulations with very low sediment availability, reaches with slopes of 0.0001 m/m or lower consistently tended to become alluvial (Figure 7). While reach-scale studies have shown that alluvial cover depends primarily on the local supply-to-capacity ratio (Chatanantavet & Parker, 2008), our network-scale perspective demonstrates how sediment redistribution across the network can maintain alluvial cover in low-slope reaches even when overall sediment supply is low.

While slope controlled the spatial distribution of alluvial cover, particularly in supply-limited conditions, the overall extent of alluvial cover was highly sensitive to changes in sediment supply and discharge. As sediment supply increased within supply-limited conditions, reaches with greater bedrock slopes became progressively covered, indicating that sediment supply controlled the extent of alluvial cover, while bedrock slope controlled its spatial distribution. These observations align with reach-scale flume experiments that reported a positive correlation between sediment flux and alluvial cover extent (Chatanantavet & Parker, 2008; Johnson & Whipple, 2010; Papangelakis et al., 2021). However, our network-scale approach found a critical transition: in transport-limited conditions, where sediment availability exceeded the network's transport capacity, the underlying bedrock slope exerted less influence on the spatial distribution of alluvial cover. Increasing sediment supply above the network's transport capacity led to the formation of new alluvial cover in reaches with similar underlying bedrock slopes to existing alluvial reaches, rather than alluvial cover developing on steeper bedrock slopes. This shift signifies a move towards a system in which sediment cover dynamics are controlled more by

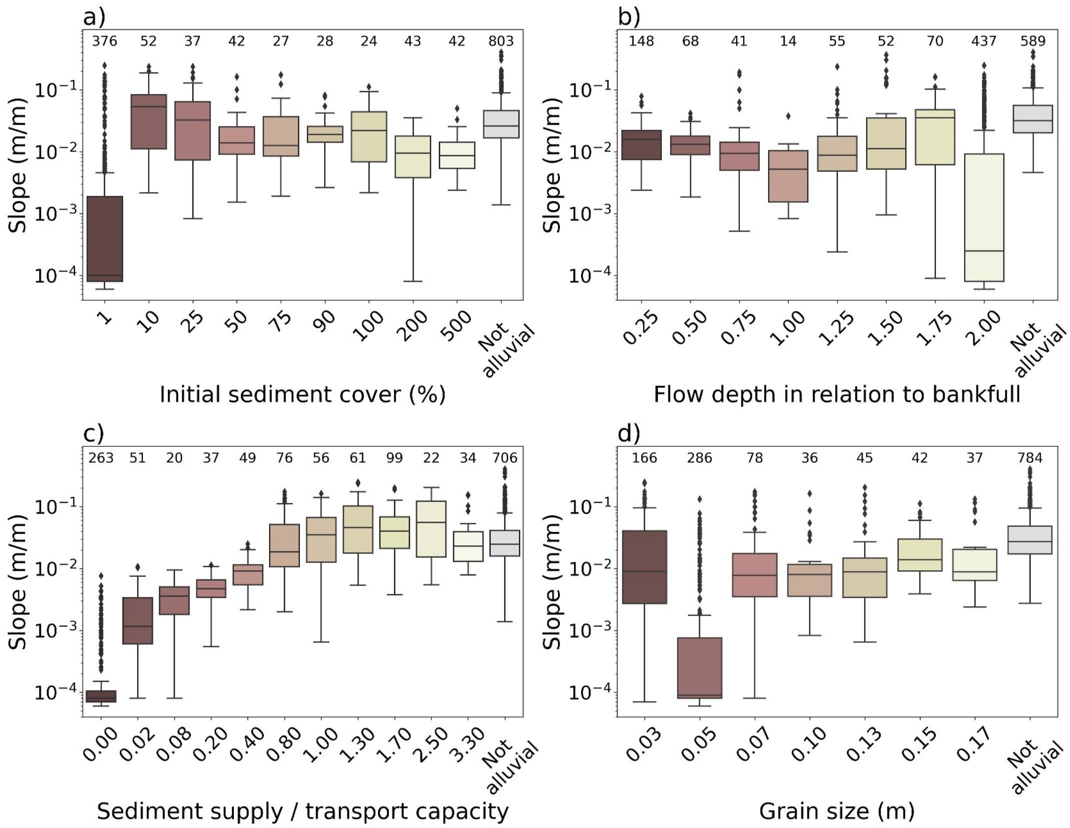

Figure 8. Box plot of channel slopes for newly formed alluvial reaches (i.e., cover fraction >99%) at steady state under varying parameters: (a) initial sediment cover; (b) flow depth relative to bankfull depth; (c) sediment supply relative to transport capacity; and (d) grain size. Each box plot represents the slopes of new alluvial reaches formed in the specific simulation compared with the previous simulation with lower parameter values. The simulations with 1% initial sediment cover, 2 times bankfull flow depth, no sediment supply, or 0.03 m grain size represent extreme conditions where fewest river segments achieved alluvial cover. The numbers at the top of each box plot indicate the number of new alluvial reaches formed in that specific simulation. The color of each box indicates the threshold value of the parameter required for that reach to become alluvial: darker colors represent lower threshold values (i.e., reach that become alluvial more easily), while lighter colors represent higher threshold values. The "Not alluvial" box (in gray) shows the slopes of the reaches that never achieved an alluvial state across all simulations.

sediment availability than by the underlying bed topography. Understanding this transition from slope-controlled to sediment supply-controlled dynamics can improve predictions of landscape evolution in mixed bedrock-alluvial river networks (e.g., Lague, 2010; Shobe et al., 2017; Zhang et al., 2015) by incorporating the spatial variability and process interactions observed at the network scale.

Additionally, in transport-limited conditions, the overall extent of alluvial cover became less sensitive to changes in sediment supply and discharge. Our simulations revealed a threshold behavior in the influence of flow depth on alluvial cover extent (Figure 4). The effect of sediment supply was more complex: while the overall increase in alluvial cover with sediment supply was gradual (Figure 4), there was a threshold behavior in its influence on the extent of bedrock and mixed reaches (Figure 3c). In supply-limited conditions, alluvial cover was highly sensitive to changes in flow depth, while the formation of bedrock and mixed reaches was primarily controlled by sediment supply. However, in transport-limited conditions, further increases in flow depth and sediment supply resulted in marginal changes in alluvial cover extent, suggesting the river's sediment transport had approached maximum efficiency. This non-linear response indicates two distinct regimes: a supply-limited space where the extent of bedrock and alluvial reaches are highly sensitive to changes in controlling parameters, and a transport-limited space where sensitivity is decreased. These findings indicate that both the magnitude of channel parameters and the regime in which variation occurs affect alluvial and bedrock distributions.

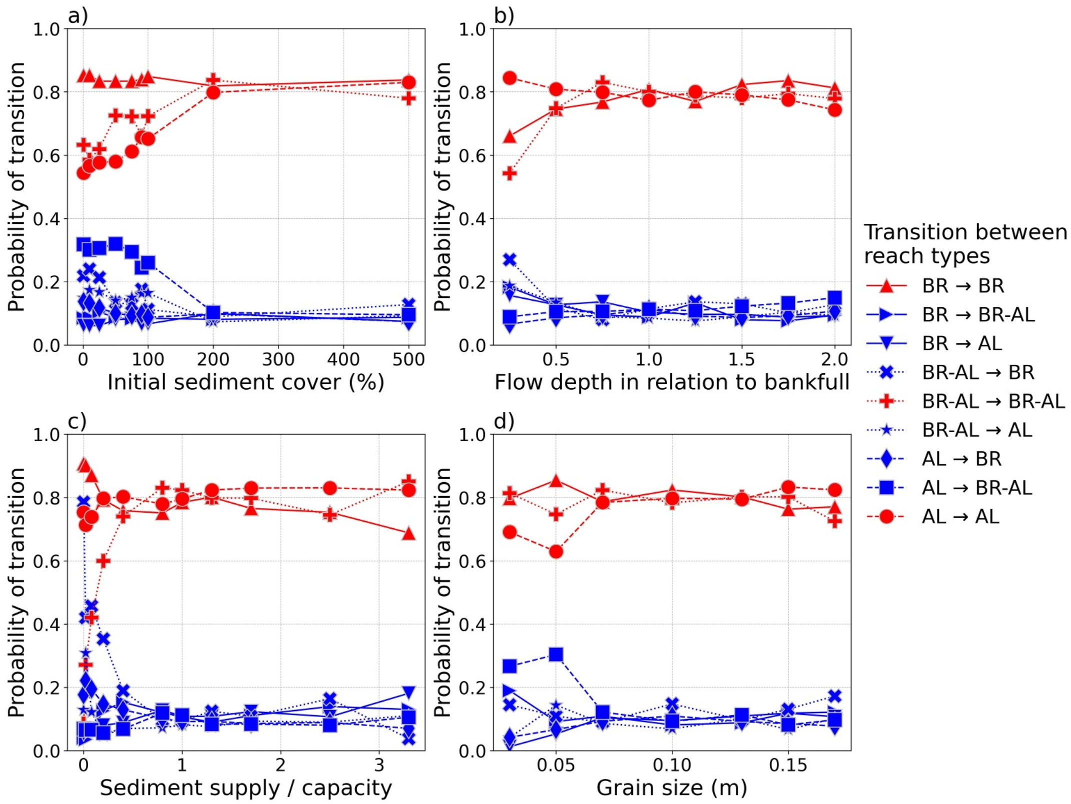

Figure 9. Probability of transition of cover categories between adjacent reaches of 100 m for each simulation that varied the parameters: (a) initial sediment cover; (b) flow depth relative to bankfull depth; (c) sediment supply relative to transport capacity; and (d) grain size. In the legend, "BR" denotes bedrock reaches with <10% cover; "BR-AL" represents mixed bedrock-alluvial reaches with 10%–99% cover; "AL" denotes alluvial reaches with >99% cover. The colors demonstrate the continuity between the same cover (in red) and the change to another cover type (in blue).

Even at sediment supply rates exceeding three times the average network's transport capacity, our results show that a fully alluviated bed did not develop across the network. This finding contradicts reach scale analyses (e.g., Chatanantavet & Parker, 2008; Cho & Nelson, 2024) that achieved full alluviation under high sediment supply. In our network-scale model, individual reaches can remain supply-limited even when overall sediment supply exceeds the network's transport capacity due to the varying slope distribution within the network. The River Carron, with slopes ranging from 0.0004 to 0.4 m/m, exemplifies this variability (Figure 1). Consequently, both supply-limited and transport-limited reaches coexist within the network, preventing complete alluviation despite a high overall sediment supply. This result suggests limitations in the system's capacity to distribute sediment effectively and indicates that river channels can maintain a mixed bedrock-alluvial state over long periods. The persistence of bedrock exposure despite high sediment supply rates challenges assumptions of complete alluviation, necessitating models to capture such non-linear dynamics at the network scale.

Table 2
Probability of Transition Matrix of Cover Type From One Reach to the Next Reach Downstream for the Default Simulation

From/to	BR	BR-AL	AL	n
BR	0.82	0.08	0.10	498
BR-AL	0.09	0.84	0.07	505
AL	0.10	0.10	0.80	511

Note. This matrix shows the probability of transitioning from one cover type (rows) to another (columns) in adjacent downstream reaches. "AL" stands for alluvial, "BR-AL" for mixed bedrock-alluvial, and "BR" for bedrock reaches. The "n" column indicates the number of reaches each type in the network.

5.2. Connectivity and Fragmentation of Alluvial Cover

Our simulations indicate that channel slope significantly influences alluvial cover connectivity, particularly under supply-limited conditions. The distribution of slopes within the network controls the fragmentation of alluvial reaches. Clusters of gentler slopes support more continuous cover, whereas networks with interspersed steep and gentle slopes result in more fragmented alluvial cover (Figures 7 and 8). Among the parameters analyzed in this study, we found that sediment supply particularly affects the connectivity of bedrock sections, with long bedrock sections under low sediment supply conditions

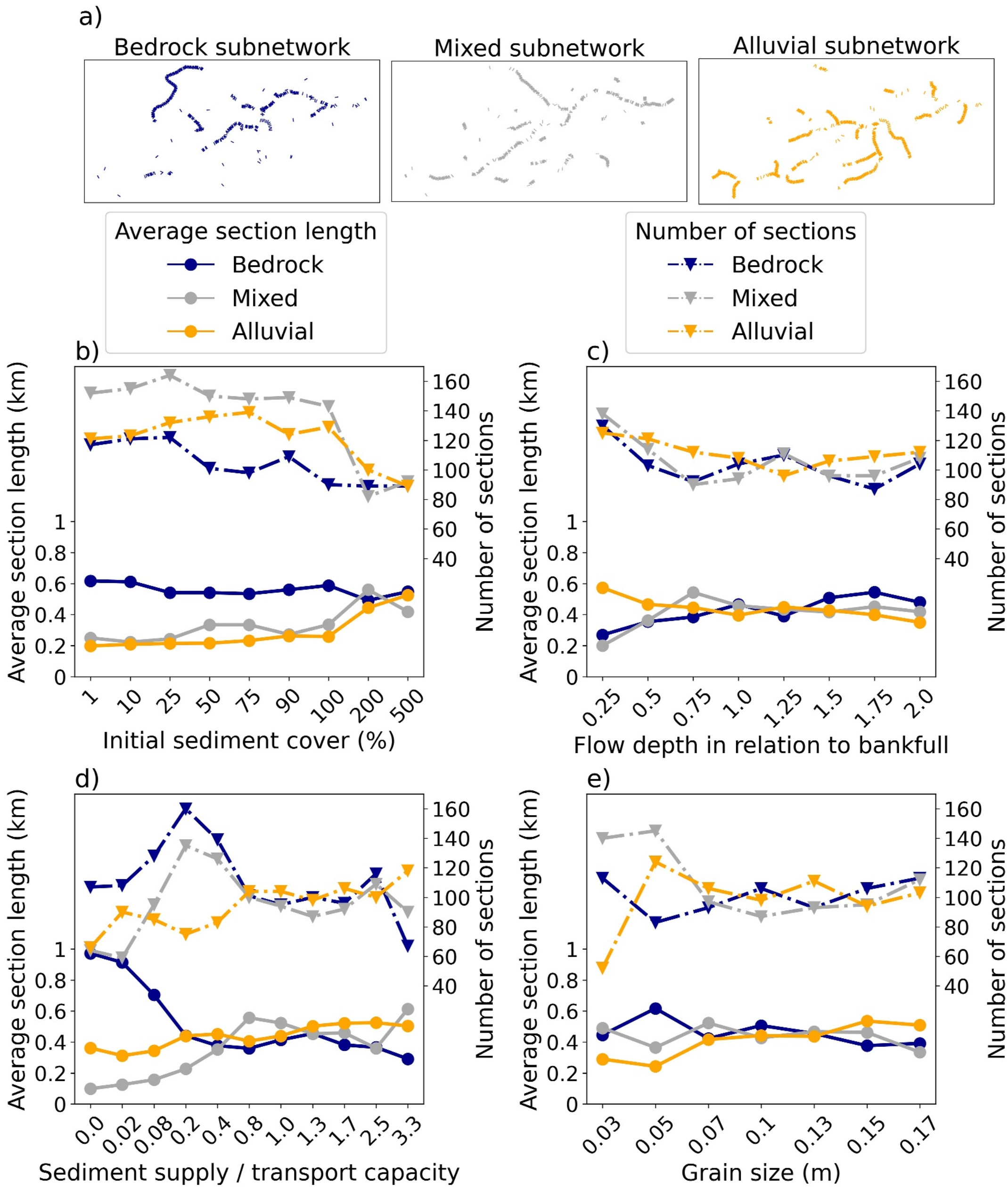

Figure 10. Length and fragmentation of cover sections. (a) Examples of subnetworks for each cover category (bedrock, mixed, or alluvial) from the default simulation. Variation in average section length and number of sections of each cover category under different simulations that varied the following parameters: (b) initial sediment cover; (c) flow depth relative to bankfull depth; (d) sediment supply relative to transport capacity; and (e) grain size.

(Figure 10). As sediment supply increased, the fragmentation of alluvial and mixed sections decreased, resulting in longer average covered lengths. Therefore, we observed a transition from slope-controlled to supply-controlled alluvial connectivity as sediment supply increased above the network's transport capacity. This finding extends previous research by demonstrating how slope and sediment supply vary across a river network. While studies such as Massong and Montgomery (2000) and Whitbread et al. (2015) also identified slope as an important factor in alluvial distribution through field data analyses, our simulations verify the effect of hydraulic and sediment supply dynamics in alluvial cover connectivity under various conditions. However, channel width and lithology, not included in our model, could also influence alluvial cover patterns. While wider channels often support more extensive alluvial cover (Massong & Montgomery, 2000; Whitbread, 2015), some studies did not find this

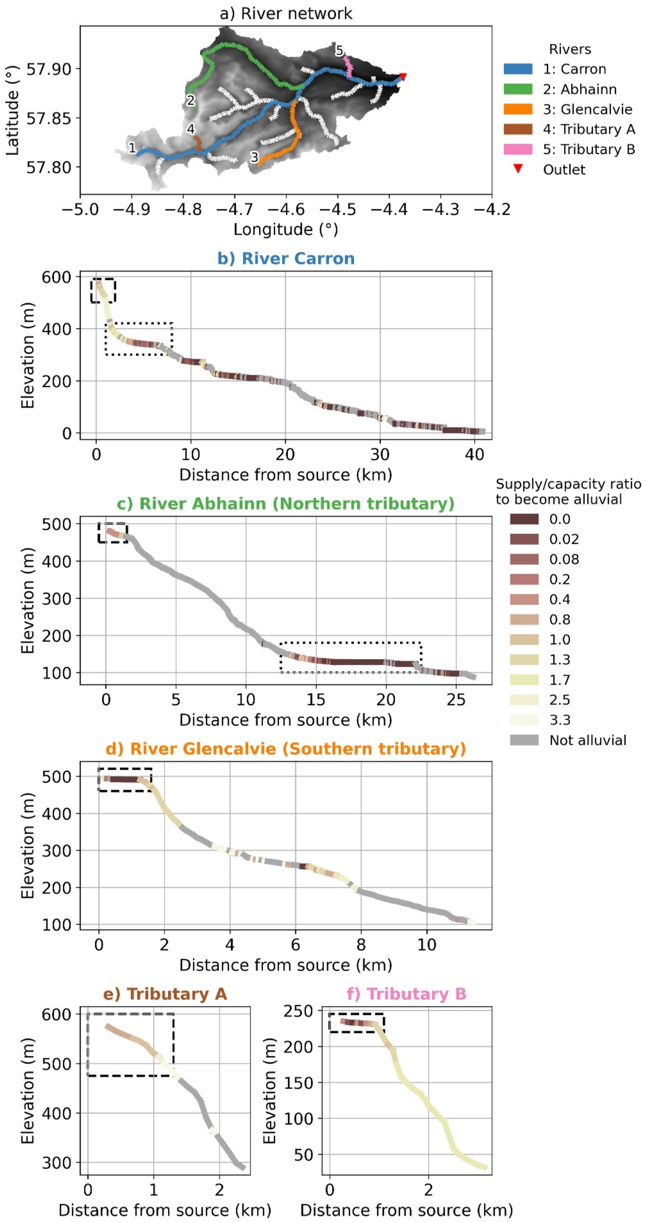

Figure 11. Longitudinal river profiles showing the sediment supply to transport capacity ratio required for reaches to become alluvial. (a) Location of the river profiles analyzed. River profiles of: (b) main river Carron; (c) northern tributary Abhainn; (d) southern tributary Glencalvie; (e) small tributary A; and (f) small tributary B. Colors indicate the minimum supply/capacity ratio at which each reach becomes fully alluvial (>99% cover), with darker colors representing reaches that become alluvial at lower supply/capacity rations and lighter colors require higher rations. Gray indicates reaches that never become fully alluvial in our simulations. Dashed boxes indicate areas where alluvial cover extends downstream as sediment supply increases and dotted boxes indicate upstream alluvial expansion as sediment supply increases. Note that the downstream expansions near headwater nodes were influenced by the proximity of the sediment supply location.

relation (Buckley et al., 2024; Montgomery & Gran, 2001). Lithology can also affect channel geometry and sediment availability (Buckley et al., 2024; Massong & Montgomery, 2000), potentially modifying the distribution and connectivity of alluvial sections across the network.

Longitudinal profile analysis (Figure 11) demonstrated that the direction of alluvial cover expansion is controlled by local slope patterns. Alluvial patches initially form in low slope sections and tend to expand in the direction of increasing bed gradient. This results in downstream expansion in convex sections and upstream expansion in concave sections as sediment supply and grain size increase or discharge decreases. This slope dependence could be used to predict the location of expansion or reduction of alluvial cover, depending on the variation of channel parameters. Therefore, slope is important for identifying hotspots of potential alluvial cover changes. Identifying such hotspots based on slope aligns with the approach used by Czuba and Foufoula-Georgiou (2015), who mapped geomorphic change hotspots based on where sediment accumulates and persists over time. Our study suggests that these areas of accumulation can be predicted by slope patterns in the network.

Persistent and elongated alluvial sections have important implications for habitat conservation and landscape evolution dynamics. Continuous alluvial sections act as storage zones, temporarily retaining sediment and delaying its downstream transfer. This sediment delay affects the connectivity and timing of sediment fluxes through the network, potentially decoupling upstream sediment sources from downstream transport and deposition patterns. In contrast, extensive bedrock sections promote rapid sediment flux, enhancing downstream connectivity and being more susceptible to active incision, thus controlling landscape evolution. Stable alluvial patches have significant ecological implications as they create diverse habitats by varying substrate composition, supporting a wide range of species (Buffington et al., 2004; Steiger et al., 2005; Wohl, 2015). In contrast, bedrock patches limit habitat diversity and are often unsuitable for spawning habitats of certain species, such as salmonids, due to high transport capacity and low sediment availability (Buffington et al., 2004). Therefore, understanding the distribution of bedrock and alluvial patches is crucial for predicting habitat availability and quality within river networks.

The transition probability matrix (Table 2) revealed a high likelihood of reaches maintaining their cover type (bedrock, mixed, or alluvial) over consecutive 100-m segments under default conditions. To the best of our knowledge, this method provides a novel approach for quantifying and comparing the spatial dynamics of alluvial cover across different mixed bedrock-alluvial river networks. Transition probability matrices have been used to explore the spatiotemporal evolution of land use and cover (Keshtkar & Voigt, 2016; Nath et al., 2020), soil cover (Liu et al., 2016), and urban areas (Silver & Silva, 2021). Further applications of this approach in mixed bedrock-alluvial rivers would require constructing transition matrices for different river networks to evaluate if these probabilities are specific for each site or share common patterns across different environments. Constructing similar matrices for other river networks could reveal common patterns in cover dynamics linked to factors, such as regional climate, tectonic regimes, or lithological characteristics. If consistent patterns emerge, transition probabilities from the studied networks could potentially be applied to similar river systems; if not, site-specific matrices would need to be developed. While the transition probability matrix could serve as an input for predictive modeling of alluvial cover evolution, it does not represent physical processes and may not account for fundamental changes under different conditions. In contrast, using slope patterns to predict alluvial cover evolution considers fundamental physical dynamics but might oversimplify by not considering other influencing factors captured by the transition matrix. Combining both approaches could be most effective in predicting alluvial cover dynamics: using slope patterns as the primary predictor and refining the predictions with the transition probability matrix.

5.3. Modeling Alluvial Cover Dynamics: Reach and Network Scales

The modeling approach employed in this study demonstrated strengths and limitations in capturing patterns of alluvial cover in mixed bedrock-alluvial river systems depending on the scale analyzed. The model satisfactorily simulated broad patterns of sediment connectivity and alluvial distribution at the network scale, revealing how changes in upstream sediment supply or flow regimes can propagate through the network and affect downstream sediment dynamics. However, although the overall model accuracy was high, the modeled sediment cover fraction at any discrete location showed substantial variance compared to the field data (Figures 2d and 2e). This indicates that the model's accuracy at discrete locations was limited. Importantly, the model results presented fluctuating alluvial cover in approximately 30% of the reaches even under steady state conditions. These fluctuations, however, did not impact overall accuracy metrics, as they mostly occurred within reaches that remained consistently alluvial, reflecting variations in sediment depth rather than transitions between bedrock and alluvial states. Fluctuation timescales varied: 43% of reaches exhibited medium-period fluctuations (10–50 timesteps), while 28% and 29% showed shorter (<10 timesteps) or longer (>50 timesteps) periodic behavior, respectively. The magnitude of these fluctuations was substantial and variable, with sediment cover typically varying by a factor of 3 during the steady state and up to a factor of 57 in the most variable reaches. The fluctuations may indicate reaches with observed inconsistent cover over time in the River Carron. Consequently, point-by-point comparisons between model results and field data should be interpreted with caution, considering the potential for temporal variability in cover in real river systems.

Simplifying assumptions in the simulation's setup may have limited its capacity to represent alluvial cover distribution at the reach scale. A simplification was not representing temporal fluctuations in discharge, thus simplifying local sediment transport and deposition patterns. Incorporating realistic flow variability would influence the predicted alluvial cover patterns, depending on the timing and magnitude of high-flow events (DeLisle & Yanites, 2023; Lague et al., 2005; Turowski et al., 2013). The steady-state conditions observed in our simulations might not be achieved under variable flow conditions. Comparing our high and low flow simulations demonstrate: the low flow simulation resulted in longer alluvial cover (53% network covered) and steeper alluvial reaches (average covered slope 0.0045 m/m) compared to the high flow simulation (29% network covered, average covered slope 0.00015 m/m) (Figures 4 and 7). In addition, the system took longer to achieve steady state under low flow conditions. These observations indicate that alluvial cover would oscillate under variable flow conditions, with intermediate slopes being particularly sensitive to flow changes. Moreover, it is uncertain whether high flow conditions would persist long enough in the field for the network sediment cover to fully adjust, potentially leading to transient rather than steady-state conditions.

Another simplification was estimating channel width based on catchment area, which does not account for potential narrowing in bedrock sections and changes in local hydraulics and transport capacity. This could result in an underestimation of shear stress and hence, overestimation of sediment deposition in bedrock reaches, particularly under low flow conditions. Additionally, our model assumes a uniform bed elevation within each reach, not accounting for macroroughness or sub-grid variations in bed topography that can influence local sediment deposition patterns (Inoue et al., 2014; Zhang et al., 2015). Furthermore, using a uniform critical shear stress regardless of the amount of alluvial cover simplified the model. In reality, bedrock reaches with smoother surfaces have lower critical shear stresses compared to alluvial surfaces (Ferguson, Sharma, Hardy et al., 2017; Ferguson, Sharma, Hodge et al., 2017; Hodge et al., 2011). Our simulations neglected the effect of sand fraction on reference shear stress, although this may be justified for the Carron network where sand content is low (Supporting Information S1). Models that account for different critical shear stress depending on cover found "runaway alluviation", a rapid transition from bedrock to alluvial conditions when sediment supply exceeds transport capacity (Chatanantavet & Parker, 2008; Cho & Nelson, 2024). Including these local variations in sediment entrainment would modify the relationship between sediment supply and alluvial cover found in our study, possibly inhibiting the formation of alluvial cover in bedrock reaches under low flow conditions or resulting in more sediment cover development on steeper slopes under high sediment supply. Variations in flow, width, sediment supply, sediment entrainment and grain size distribution were not included in our simulations due to the increased complexity of our network-scale modeling; however, they are important areas for future model development to improve reach-scale predictions of this network model.

Additional limitations of our model approach include the extensive computational time required to achieve complete steady state conditions across the entire network (up to 2 weeks of CPU time) and the simplified representation of sediment supply locations. The complex interaction of sediment routing, storage and channel slope adjustment in the network can lead to long transient states with apparently stable conditions, making it computationally challenging to reach a fully stabilized network. Our model introduced sediments only at headwater reaches, which does not represent lateral sediment input from hillslopes to rivers throughout the network. This approach may have led to an overestimation of transport capacity relative to sediment supply in downstream reaches, potentially decreasing alluvial cover with distance downstream. These factors can influence the spatial distribution of alluvial cover, particularly by creating more supply-limited conditions in downstream areas. Future applications of this model could benefit from incorporating distributed sediment inputs along the network to better represent hillslope contributions and improve the representation of sediment dynamics in downstream reaches. Further exploration of these aspects, including a comparison between our results and a simplified zero-order model based on transport capacity, is provided in the Supporting Information S1. This comparison showed that the zero-order model predicted more alluvial reaches than our simulations, particularly under high sediment supply conditions, demonstrating the complex sediment routing, storage dynamics and temporal evolution represented by the NetworkSedimentTransporter model.

Despite these simplifications, our model provides insights that could enhance landscape evolution models (LEMs). Traditional LEMs represent the fundamental processes of fluvial incision into bedrock and sediment transport that shape landscapes over geological timescales (Howard, 1994; Whipple & Tucker, 2002). However, these models often simplify or ignore the fine-scale dynamics of sediment cover distribution and the transitions between bedrock and alluvial states within river networks. Our results show that bedrock sections persist even under high sediment supply conditions and that the formation of alluvial reaches can decouple sediment connectivity along the network. These results demonstrate the complexity of transitioning between bedrock and alluvial channel states, and that stable bedrock reaches can persist and erode for a long time despite variations in sediment supply. Detachment-limited LEMs assume an erosion framework, where sediment is readily evacuated from the system (e.g., Howard, 1994). These LEMs may not capture the decoupled sediment dynamics and the coexistence of bedrock and alluvial sections under different sediment regimes. Even transport-limited LEMs, which account for simple sediment transport dynamics (e.g., Willgoose et al., 1991), may fail to recreate the observed coexistence of bedrock and alluvial sections under different sediment regimes, as they often assume more uniform sediment cover conditions. Some recent LEMs, such as SPACE (Shobe et al., 2017), are capable of modeling cover dynamics and the coexistence of bedrock and alluvial reaches. However, our network-scale approach using NetworkSedimentTransporter offers additional insights. For example, our model can incorporate variability in grain size, which is not present in SPACE, and focuses on network-scale connectivity and spatial distribution of alluvial cover. These features could provide a more detailed understanding of how sediment routing affects landscape volution.

The alluvial cover model on a network scale used in this study could be integrated into LEMs to enhance their capabilities, such as the persistence and erosion of bedrock sections. An approach is to develop a bed cover evolution sub-model for LEMs that incorporates detailed alluvial cover spatial distribution and connectivity dynamics, building upon existing models such as SPACE (Shobe et al., 2017). This sub-model uses inputs from LEMs, such as topography, discharge, and sediment supply, to calculate the spatial patterns of alluvial cover within the river network. The outputs could then be integrated into the LEMs' erosion and sediment transport calculations, allowing them to capture the influence of these finer-scale sediment dynamics on larger-scale landscape evolution processes. This coupling could improve the predictive capabilities of LEMs in mixed bedrock-alluvial river systems by accounting for the feedback between alluvial cover dynamics, sediment connectivity, and broader landscape evolution processes.

6. Conclusion

This study combined network scale modeling and connectivity analysis to investigate the complex interactions between primary controls on alluvial cover within a mixed bedrock-alluvial river network. Previous research has focused on reach-scale analysis, while network-scale studies have been limited. We assessed the effects of changing sediment supply, flow depth, and grain size on cover transitions, fragmentation, and expansion of alluvial, mixed and bedrock sections on a network scale.

The results of this study have implications for understanding how mixed bedrock-alluvial systems respond to environmental changes. First, the spatial distribution of alluvial cover was strongly controlled by slope, particularly in supply-limited conditions. However, as sediment supply increased and the system shifted to transport-limited conditions, the influence of slope on spatial distribution decreased, while the effects of sediment supply and grain size became more significant. Second, the extent of alluvial cover was more responsive to changes in sediment supply and discharge in supply-limited conditions compared to transport-limited conditions. This indicates that in supply-limited settings, minor variations in sediment input or discharge can lead to substantial changes in the overall alluvial cover extent, while in transport-limited conditions, the system becomes less responsive to these changes. Third, even at sediment supply rates significantly exceeding the network's transport capacity, not all reaches achieved full alluviation. This suggests inherent limitations in the system's ability to distribute and retain sediment uniformly across the network. Finally, channel slope can potentially be used to predict hotspots of alluvial cover change, with alluvial sections expanding in the direction of increasing slope. Determining these hotspots has implications for predicting habitat availability and quality within river networks. It is important to note that our model assumptions, such as uniform grain size and sediment supply only at headwater reaches, may have affected our findings by simplifying the complex sediment dynamics found in natural systems.

Future research could focus on key areas to further improve the understanding of alluvial cover dynamics in mixed bedrock-alluvial river systems. First, incorporating more detailed reach-scale processes into landscape evolution models (LEMs) could improve the accuracy in representing alluvial cover dynamics. Traditional LEMs often simplify fine-scale sediment cover transitions and could more accurately simulate these processes, such as the persistence of bedrock sections under high sediment supply found in this study. Second, more research is needed on how the spatial extent and dynamics of alluvial cover change during perturbations to river networks, such as extreme storm events or sediment pulses from landsliding. Third, empirical studies of sediment cover variations throughout river networks in different environments are needed to validate and refine modeling approaches. Some challenges include the need for high-resolution data, increased computational demands, and accurately representing localized hydraulic and sediment transport processes within river network models. Despite these challenges, the potential benefits include improving river management, conservation strategies, and the predictive capabilities of landscape evolution models.

Data Availability Statement

The river data used for model input and evaluation are available in Whitbread (2015) and Whitbread et al. (2015). Grain size and sediment cover data collected during this study and used in the model are available in Guirro et al. (2025). The NetworkSedimentTransporter model used for simulating sediment transport and alluvial cover in the river network is freely accessible in Python as detailed in Pfeiffer et al. (2020) and developed openly by the Landlab team (https://github.com/landlab/landlab). The LSDTopoTools topographic analysis software used to delineate the river network is freely available at Mudd et al. (2023).

Acknowledgments
This research is a part of the "i-CONN" project funded by the European Union's Horizon 2020 research and innovation programme under the Marie Skłodowska-Curie grant agreement number 859937. We would like to thank Jennifer King for her assistance during field work, the Landlab team and Earth Surface Processes Institute (ESPIn) for their support in learning and using the NetworkSedimentTransporter, and Bruno Cheviron for his valuable discussions about the sensitivity analysis. We also thank the reviewers for their constructive feedback, which contributed to enhancing the quality of this manuscript.

References

Ahammad, M., Czuba, J. A., Pfeiffer, A. M., Murphy, B. P., & Belmont, P. (2021). Simulated dynamics of mixed versus uniform grain size sediment pulses in a gravel-bedded river. *Journal of Geophysical Research: Earth Surface*, *126*(10), e2021JF006194. https://doi.org/10.1029/2021JF006194

Ballantyne, C. K. (2008). After the ice: Holocene geomorphic activity in the Scottish Highlands. *Scottish Geographical Journal*, *124*(1), 8–52. https://doi.org/10.1080/14702540802300167

Baynes, E. R. C., Lague, D., Steer, P., Bonnet, S., & Illien, L. (2020). Sediment flux-driven channel geometry adjustment of bedrock and mixed gravel–bedrock rivers. *Earth Surface Processes and Landforms*, *45*(14), 3714–3731. https://doi.org/10.1002/esp.4996

Bizzi, S., Tangi, M., Schmitt, R. J. P., Pitlick, J., Piégay, H., & Castelletti, A. F. (2021). Sediment transport at the network scale and its link to channel morphology in the braided Vjosa River system. *Earth Surface Processes and Landforms*, *46*(14), 2946–2962. https://doi.org/10.1002/esp.5225

Bracken, L. J., Turnbull, L., Wainwright, J., & Bogaart, P. (2015). Sediment connectivity: A framework for understanding sediment transfer at multiple scales: Sediment connectivity: Sediment transfer at multiple scales. *Earth Surface Processes and Landforms*, *40*(2), 177–188. https://doi.org/10.1002/esp.3635

British Geological Survey. (2008). BGS geology 625K. Retrieved from https://www.bgs.ac.uk/datasets/bgs-geology-625k-digmapgb/

Buckley, J., Hodge, R. A., & Slater, L. J. (2024). Bedrock rivers are steep but not narrow: Hydrological and lithological controls on river geometry across the USA. *Geology*, *52*(7), 522–526. https://doi.org/10.1130/G51627.1

Buffington, J. M., Montgomery, D. R., & Greenberg, H. M. (2004). Basin-scale availability of salmonid spawning gravel as influenced by channel type and hydraulic roughness in mountain catchments. *Canadian Journal of Fisheries and Aquatic Sciences*, *61*(11), 2085–2096. https://doi.org/10.1139/f04-141

Chatanantavet, P., & Parker, G. (2008). Experimental study of bedrock channel alluviation under varied sediment supply and hydraulic conditions: Experiments. *Water Resources Research*, *44*(12), W12446. https://doi.org/10.1029/2007WR006581

Cho, J., & Nelson, P. A. (2024). Patterns of alluviation in mixed bedrock-alluvial channels: 2. Controls on the formation of alluvial patches. *Journal of Geophysical Research: Earth Surface*, *129*(1), e2023JF007293. https://doi.org/10.1029/2023JF007293

Cook, K. L., Turowski, J. M., & Hovius, N. (2020). Width control on event-scale deposition and evacuation of sediment in bedrock-confined channels. *Earth Surface Processes and Landforms*, *45*(14), 3702–3713. https://doi.org/10.1002/esp.4993

Czuba, J. A. (2018). A Lagrangian framework for exploring complexities of mixed-size sediment transport in gravel-bedded river networks. *Geomorphology*, *321*, 146–152. https://doi.org/10.1016/j.geomorph.2018.08.031

Czuba, J. A., & Foufoula-Georgiou, E. (2014). A network-based framework for identifying potential synchronizations and amplifications of sediment delivery in river basins. *Water Resources Research*, *50*(5), 3826–3851. https://doi.org/10.1002/2013WR014227

Czuba, J. A., & Foufoula-Georgiou, E. (2015). Dynamic connectivity in a fluvial network for identifying hotspots of geomorphic change. *Water Resources Research*, *51*(3), 1401–1421. https://doi.org/10.1002/2014WR016139

Czuba, J. A., Foufoula-Georgiou, E., Gran, K. B., Belmont, P., & Wilcock, P. R. (2017). Interplay between spatially explicit sediment sourcing, hierarchical river-network structure, and in-channel bed material sediment transport and storage dynamics. *Journal of Geophysical Research: Earth Surface*, *122*(5), 1090–1120. https://doi.org/10.1002/2016JF003965

DeLisle, C., & Yanites, B. J. (2023). Rethinking variability in bedrock rivers: Sensitivity of hillslope sediment supply to precipitation events modulates bedrock incision during floods. *Journal of Geophysical Research: Earth Surface*, *128*(9), e2023JF007148. https://doi.org/10.1029/2023JF007148

Ferguson, R. I., Sharma, B. P., Hardy, R. J., Hodge, R. A., & Warburton, J. (2017a). Flow resistance and hydraulic geometry in contrasting reaches of a bedrock channel: Bedrock flow resistance. *Water Resources Research*, *53*(3), 2278–2293. https://doi.org/10.1002/2016WR020233

Ferguson, R. I., Sharma, B. P., Hodge, R. A., Hardy, R. J., & Warburton, J. (2017b). Bed load tracer mobility in a mixed bedrock/alluvial channel: Tracer-Pebble Mobility over Bedrock. *Journal of Geophysical Research: Earth Surface*, *122*(4), 807–822. https://doi.org/10.1002/2016JF003946

Finnegan, N. J., Klier, R. A., Johnstone, S., Pfeiffer, A. M., & Johnson, K. (2017). Field evidence for the control of grain size and sediment supply on steady-state bedrock river channel slopes in a tectonically active setting: Grain size and steady-state bedrock river channel slopes. *Earth Surface Processes and Landforms*, *42*(14), 2338–2349. https://doi.org/10.1002/esp.4187

Fryirs, K. (2013). (Dis)Connectivity in catchment sediment cascades: A fresh look at the sediment delivery problem: (Dis)connectivity in catchment sediment cascades. *Earth Surface Processes and Landforms*, *38*(1), 30–46. https://doi.org/10.1002/esp.3242

Goode, J. R., & Wohl, E. (2010). Coarse sediment transport in a bedrock channel with complex bed topography. *Water Resources Research*, *46*(11), 2009WR008135. https://doi.org/10.1029/2009WR008135

Gran, K. B., & Czuba, J. A. (2017). Sediment pulse evolution and the role of network structure. *Geomorphology*, *277*, 17–30. https://doi.org/10.1016/j.geomorph.2015.12.015

Guirro, M. O., Hodge, R., Clubb, F., & Turnbull, L. (2025). Sediment cover and grain size data for the River Carron Catchment, Scotland (2022) [Dataset]. *Zenodo*. https://doi.org/10.5281/zenodo.14826181

Hagberg, A. A., Schult, D. A., & Swart, P. J. (2008). Exploring network structure, dynamics, and function using NetworkX. In G. Varoquaux, T. Vaught, & J. Millman (Eds.), *Proceedings of the 7th Python in Science Conference (SciPy2008)* (pp. 11–15).

Hodge, R. A., & Hoey, T. B. (2016). A froude-scaled model of a bedrock-alluvial channel reach: 2. Sediment cover: Bedrock-alluvial model: Sediment. *Journal of Geophysical Research: Earth Surface*, *121*(9), 1597–1618. https://doi.org/10.1002/2015JF003709

Hodge, R. A., Hoey, T. B., & Sklar, L. S. (2011). Bed load transport in bedrock rivers: The role of sediment cover in grain entrainment, translation, and deposition. *Journal of Geophysical Research*, *116*(F4), F04028. https://doi.org/10.1029/2011JF002032

Howard, A. D. (1994). A detachment-limited model of drainage basin evolution. *Water Resources Research*, *30*(7), 2261–2285. https://doi.org/10.1029/94WR00757

Inoue, T., Izumi, N., Shimizu, Y., & Parker, G. (2014). Interaction among alluvial cover, bed roughness, and incision rate in purely bedrock and alluvial-bedrock channel. *Journal of Geophysical Research: Earth Surface*, *119*(10), 2123–2146. https://doi.org/10.1002/2014JF003133

Jafarinik, S., & Viparelli, E. (2020). Alluvial morphodynamics of low-slope bedrock reaches transporting nonuniform bed material. *Water Resources Research*, *56*(10), e2020WR027345. https://doi.org/10.1029/2020WR027345

Johnson, J. P. L. (2014). A surface roughness model for predicting alluvial cover and bed load transport rate in bedrock channels: Bedrock roughness alluvial cover model. *Journal of Geophysical Research: Earth Surface*, *119*(10), 2147–2173. https://doi.org/10.1002/2013JF003000

Johnson, J. P. L., & Whipple, K. X. (2010). Evaluating the controls of shear stress, sediment supply, alluvial cover, and channel morphology on experimental bedrock incision rate: Stress, sediment supply, and alluviation. *Journal of Geophysical Research*, *115*(F2), F02018. https://doi.org/10.1029/2009JF001335

Keshtkar, H., & Voigt, W. (2016). A spatiotemporal analysis of landscape change using an integrated Markov chain and cellular automata models. *Modeling Earth Systems and Environment*, *2*(1), 10. https://doi.org/10.1007/s40808-015-0068-4

Lague, D. (2010). Reduction of long-term bedrock incision efficiency by short-term alluvial cover intermittency. *Journal of Geophysical Research*, *115*(F2), F02011. https://doi.org/10.1029/2008JF001210

Lague, D., Hovius, N., & Davy, P. (2005). Discharge, discharge variability, and the bedrock channel profile. *Journal of Geophysical Research*, *110*(F4), 2004JF000259. https://doi.org/10.1029/2004JF000259

Liu, R., Men, C., Wang, X., Xu, F., & Yu, W. (2016). Application of spatial Markov chains to the analysis of the temporal–spatial evolution of soil erosion. *Water Science and Technology*, *74*(5), 1051–1059. https://doi.org/10.2166/wst.2016.283

Massong, T. M., & Montgomery, D. R. (2000). Influence of sediment supply, lithology, and wood debris on the distribution of bedrock and alluvial channels. *Geological Society of America Bulletin*, *112*(4), 591–599. https://doi.org/10.1130/0016-7606(2000)112<0591:iossla>2.3.co;2

Meshkova, L. V., & Carling, P. A. (2013). Discrimination of alluvial and mixed bedrock-alluvial multichannel river networks: Channel metrics. *Earth Surface Processes and Landforms*, *38*(11), 1299–1316. https://doi.org/10.1002/esp.3417

Montgomery, D. R., & Gran, K. B. (2001). Downstream variations in the width of bedrock channels. *Water Resources Research*, *37*(6), 1841–1846. https://doi.org/10.1029/2000WR900393

Mudd, S. M., Clubb, F. J., Grieve, S. W. D., Milodowski, D. T., Gailleton, B., Hurst, M. D., et al. (2023). LSDtopotools/LSDTopoTools2: LSDTopoTools2 v0.9 (v0.9) [Software]. *Zenodo*. https://doi.org/10.5281/zenodo.8076231

Murphy, B. P., Czuba, J. A., & Belmont, P. (2019). Post-wildfire sediment cascades: A modeling framework linking debris flow generation and network-scale sediment routing. *Earth Surface Processes and Landforms*, *44*(11), 2126–2140. https://doi.org/10.1002/esp.4635

Nath, B., Wang, Z., Ge, Y., Islam, K., P. Singh, R., & Niu, Z. (2020). Land use and land cover change modeling and future potential landscape risk assessment using Markov-CA model and analytical hierarchy process. *ISPRS International Journal of Geo-Information*, *9*(2), 134. https://doi.org/10.3390/ijgi9020134

Ordnance Survey. (2022). *OS Terrain 5 [ASC geospatial data], scale 1:10,000, Tiles: nh59se, nh69sw*. Available from EDINA Digimap Ordnance Survey Service. Retrieved from https://digimap.edina.ac.uk

Papangelakis, E., Welber, M., Ashmore, P., & MacVicar, B. (2021). Controls of alluvial cover formation, morphology and bedload transport in a sinuous channel with a non-alluvial boundary. *Earth Surface Processes and Landforms*, *46*(2), 399–416. https://doi.org/10.1002/esp.5032

Pfeiffer, A., Barnhart, K., Czuba, J., & Hutton, E. (2020). NetworkSedimentTransporter: A Landlab component for bed material transport through river networks [Software]. *Journal of Open Source Software*, *5*(53), 2341. https://doi.org/10.21105/joss.02341

Purinton, B., & Bookhagen, B. (2019). Introducing PebbleCounts: A grain-sizing tool for photo surveys of dynamic gravel-bed rivers [Preprint]. *Physical: Geomorphology*. https://doi.org/10.5194/esurf-2019-20

Rennie, C. D., Church, M., & Venditti, J. G. (2018). Rock control of river geometry: The fraser canyons. *Journal of Geophysical Research: Earth Surface*, *123*(8), 1860–1878. https://doi.org/10.1029/2017JF004458

Schmitt, R. J. P., Bizzi, S., & Castelletti, A. (2016). Tracking multiple sediment cascades at the river network scale identifies controls and emerging patterns of sediment connectivity: Tracking multiple sediment cascades at river network scale. *Water Resources Research*, *52*(5), 3941–3965. https://doi.org/10.1002/2015WR018097

Schmitt, R. J. P., Bizzi, S., Castelletti, A., & Kondolf, G. M. (2018). Improved trade-offs of hydropower and sand connectivity by strategic dam planning in the Mekong. *Nature Sustainability*, *1*(2), 96–104. https://doi.org/10.1038/s41893-018-0022-3

Shobe, C. M., Tucker, G. E., & Barnhart, K. R. (2017). The space 1.0 model: A Landlab component for 2-D calculation of sediment transport, bedrock erosion, and landscape evolution. *Geoscientific Model Development*, *10*(12), 4577–4604. https://doi.org/10.5194/gmd-10-4577-2017

Silver, D., & Silva, T. H. (2021). A Markov model of urban evolution: Neighbourhood change as a complex process. *PLoS One*, *16*(1), e0245357. https://doi.org/10.1371/journal.pone.0245357

Sklar, L., & Dietrich, W. E. (1998). River longitudinal profiles and bedrock incision models: Stream power and the influence of sediment supply. In J. Tinkler & E. Wohl (Eds.), *Geophysical monograph series* (Vol. 107, pp. 237–260). American Geophysical Union. https://doi.org/10.1029/GM107p0237

Sklar, L. S., & Dietrich, W. E. (2004). A mechanistic model for river incision into bedrock by saltating bed load. *Water Resources Research*, *40*(6), W06301. https://doi.org/10.1029/2003WR002496

Steiger, J., Tabacchi, E., Dufour, S., Corenblit, D., & Peiry, J.-L. (2005). Hydrogeomorphic processes affecting riparian habitat within alluvial channel–floodplain river systems: A review for the temperate zone. *River Research and Applications*, *21*(7), 719–737. https://doi.org/10.1002/rra.879

Tangi, M., Schmitt, R., Bizzi, S., & Castelletti, A. (2019). The CASCADE toolbox for analyzing river sediment connectivity and management. *Environmental Modelling & Software*, *119*, 400–406. https://doi.org/10.1016/j.envsoft.2019.07.008

Toone, J., Rice, S. P., & Piégay, H. (2014). Spatial discontinuity and temporal evolution of channel morphology along a mixed bedrock-alluvial river, upper Drôme River, southeast France: Contingent responses to external and internal controls. *Geomorphology*, *205*, 5–16. https://doi.org/10.1016/j.geomorph.2012.05.033

Turowski, J. M. (2018). Alluvial cover controlling the width, slope and sinuosity of bedrock channels. *Earth Surface Dynamics*, *6*(1), 29–48. https://doi.org/10.5194/esurf-6-29-2018

Turowski, J. M., Badoux, A., Leuzinger, J., & Hegglin, R. (2013). Large floods, alluvial overprint, and bedrock erosion. *Earth Surface Processes and Landforms*, *38*(9), 947–958. https://doi.org/10.1002/esp.3341

Turowski, J. M., Hovius, N., Wilson, A., & Horng, M.-J. (2008). Hydraulic geometry, river sediment and the definition of bedrock channels. *Geomorphology*, *99*(1–4), 26–38. https://doi.org/10.1016/j.geomorph.2007.10.001

Turowski, J. M., Lague, D., & Hovius, N. (2007). Cover effect in bedrock abrasion: A new derivation and its implications for the modeling of bedrock channel morphology. *Journal of Geophysical Research*, *112*(F4), 2006JF000697. https://doi.org/10.1029/2006JF000697

Whipple, K. X., DiBiase, R. A., & Crosby, B. T. (2013). 9.28 bedrock rivers. In *Treatise on geomorphology* (pp. 550–573). Elsevier. https://doi.org/10.1016/B978-0-12-374739-6.00254-2

Whipple, K. X., & Tucker, G. E. (2002). Implications of sediment-flux-dependent river incision models for landscape evolution. *Journal of Geophysical Research*, *107*(B2). https://doi.org/10.1029/2000JB000044

Whitbread, K. (2015). Channel geometry data set for the northwest Scottish Highlands [Dataset]. https://nora.nerc.ac.uk/id/eprint/511094

Whitbread, K., Jansen, J., Bishop, P., & Attal, M. (2015). Substrate, sediment, and slope controls on bedrock channel geometry in postglacial streams [Dataset]. *Journal of Geophysical Research: Earth Surface*, *120*(5), 779–798. https://doi.org/10.1002/2014JF003295

Wilcock, P. R., & Crowe, J. C. (2003). Surface-based transport model for mixed-size sediment. *Journal of Hydraulic Engineering*, *129*(2), 120–128. https://doi.org/10.1061/(ASCE)0733-9429(2003)129:2(120)

Willgoose, G., Bras, R. L., & Rodriguez-Iturbe, I. (1991). A coupled channel network growth and hillslope evolution model: 1. Theory. *Water Resources Research*, *27*(7), 1671–1684. https://doi.org/10.1029/91WR00935

Wohl, E. (2015). Particle dynamics: The continuum of bedrock to alluvial river segments. *Geomorphology*, *241*, 192–208. https://doi.org/10.1016/j.geomorph.2015.04.014

Wong, M., Parker, G., DeVries, P., Brown, T. M., & Burges, S. J. (2007). Experiments on dispersion of tracer stones under lower-regime plane-bed equilibrium bed load transport: Flume experiments on dispersion of tracer stones. *Water Resources Research*, *43*(3), W03440. https://doi.org/10.1029/2006WR005172

Zhang, L., Parker, G., Stark, C. P., Inoue, T., Viparelli, E., Fu, X., & Izumi, N. (2015). Macro-roughness model of bedrock–alluvial river morphodynamics. *Earth Surface Dynamics*, *3*(1), 113–138. https://doi.org/10.5194/esurf-3-113-2015